

Article

Effective Thermal Conductivity and Borehole Thermal Resistance in Selected Borehole Heat Exchangers for the Same Geology

Tomasz Sliwa ^{1,*} , Patryk Leśniak ¹, Aneta Sapińska-Śliwa ¹ and Marc A. Rosen ²

¹ Laboratory of Geoenergetics, Drilling, Oil and Gas Faculty, AGH University of Science and Technology, Al. Mickiewicza 30, 30-059 Krakow, Poland; lesniakp@student.agh.edu.pl (P.L.); ans@agh.edu.pl (A.S.-Ś.)

² Faculty of Engineering and Applied Science, Ontario Tech University, Oshawa, ON L1G 0C5, Canada; marc.rosen@ontariotechu.ca

* Correspondence: sliwa@agh.edu.pl; Tel.: +48-12-617-22-17; Fax: +48-12-617-22-06

Abstract: Investigating the constructions of borehole heat exchangers with high efficiency (unit heat transfer between the heat carrier and ground) is important. One of the means to improve efficiency is the use of the most efficient construction of the borehole heat exchanger. The paper describes research on borehole heat exchangers' thermal efficiency, which is mainly characterized by parameters obtained from a thermal response test: effective thermal conductivity and borehole thermal resistivity. The borehole heat exchangers of the Laboratory of Geoenergetics in Poland were studied. Based on thermal response test interpretation and empirical equations, one of which is proprietary, the heat transfer is calculated independent of the duration of the thermal response test. Other conditions for using borehole heat exchangers in downtowns are discussed. The research aims to determine the best borehole heat exchanger design from five basic possibilities studied. A lack of unequivocal statements regarding this matter in the literature was observed. The influence of the interpretation method on the research results is determined. A single U-tube system filled with gravel is shown to be the most advantageous design by a very small margin. The applied interpretation methods, however, confirm the hitherto ambiguity in the selection of the best construction. The maximum heat carrier temperature at the end of thermal response tests was 32 °C for a geological profile mostly made up of clay (low thermal conductivity) and 23 °C for Carpathian flysch (sandstones and shales, with a higher value of conductivity).

Keywords: borehole heat exchanger; geothermal heat; borehole thermal resistance; geoenergetics; geothermal heat pump; thermal response test



Citation: Sliwa, T.; Leśniak, P.; Sapińska-Śliwa, A.; Rosen, M.A. Effective Thermal Conductivity and Borehole Thermal Resistance in Selected Borehole Heat Exchangers for the Same Geology. *Energies* **2022**, *15*, 1152. <https://doi.org/10.3390/en15031152>

Academic Editors: Efstathios E. Michaelides and Jasmin Raymond

Received: 28 June 2021

Accepted: 25 January 2022

Published: 4 February 2022

Publisher's Note: MDPI stays neutral with regard to jurisdictional claims in published maps and institutional affiliations.



Copyright: © 2022 by the authors. Licensee MDPI, Basel, Switzerland. This article is an open access article distributed under the terms and conditions of the Creative Commons Attribution (CC BY) license (<https://creativecommons.org/licenses/by/4.0/>).

1. Introduction

Heat exchangers are used to transfer heat between two or more fluids at different temperatures or between a fluid and solid particulates. Many kinds of heat exchangers are utilized globally, and they differ due to the requirements placed on them. Shell and tube, plate and shell, double pipe, plate fin, and pillow plate are some examples of the types of industrial-scale heat exchangers [1]. Factors such as fluid flow rate and type and direction of the tube flow impact the performance of a heat exchanger [1]. Heat exchanger performance factors, such as heat load, fluid temperature, effectiveness, and overall heat transfer coefficient, have been examined for various factors and operating conditions [2,3].

Research on borehole heat exchanger (BHE) fields and heat storage in the ground is progressing at numerous universities and research organizations. Some of the oldest investigations were performed in Sweden, including research at Luleå University of Technology, which installed the first large-scale borehole thermal storage in 1982–83 [4].

Apart from the work at AGH University of Science and Technology (AGH UST) in Krakow (Poland), research is ongoing in the Czech Republic at the Technical University of

Ostrava (Vysoká škola báňská). Bujok et al. [5] describe the BHE system at this university and its arrangement. A borehole thermal energy storage (BTES) system at Ontario Tech University (formerly the University of Ontario Institute of Technology), Oshawa, Canada is described by Koochi-Fayegh and Rosen [6]. Systems with geothermal heat pumps and BHEs exist among others in the Karlsruhe Institute of Technology [7], Polytechnic University of Turin [8], University of Western Ontario [9], and Ball State University [10]. A deep BHE was drilled in RWTH Aachen University (Rheinisch-Westfälische Technische Hochschule Aachen) [11].

Some of the first and most important scientific experiments and achievements in the field of geothermal heat pumps were obtained with BHEs located in Europe (Sweden [12–14], Switzerland [15,16], Germany [17,18], and Croatia [19]), in Canada [20,21], in the USA [22,23], and in Japan [24]. Currently, much research regarding BHEs is conducted in China [25].

Present research on BHEs is delving into many detailed aspects, such as:

- Material research [26].
- Depth maximization for specific BHE construction [27], in terms of the type of pipe material and rock stability.
- Utilizing old/abandoned/closed boreholes drilled for different reasons [28].
- Operational parameters optimization [29] such as the type of heat carrier, its flow rate and velocity, inlet temperature, heating power (optimized for coefficient of performance of geothermal heat pump).
- Construction type, such as single U-tube, multi-U-tube, coaxial [30,31], helical [32,33], BHE in piles [34], geothermal baskets [35], and geothermal radial drilling (GRD) [36], taking into consideration diameter and thickness of pipes [37].
- Borehole axis, noting BHEs can be drilled either vertically or directionally (obliquely) using the BHE construction technology GRD, with such wells having been drilled under buildings and town infrastructure in Pałecznicza [38].
- Cementing materials [39,40].

Other factors are also being investigated. For example, W- and coil-type heat exchangers [41]. A W-type heat exchanger is a double serial (not parallel) U-pipe in one borehole.

Ball State University, Indiana, USA has the largest BHE installation, with 3600 vertical loops. The system replaced four old coal-fired boilers and cools and heats 47 buildings by supplying 6 °C cold water for cooling and 66 °C hot water for heating. The BHE system saves USD 2 million annually [42]. BHE depths in the installation range from 122 to 152 m [22,43]. Lee [44] describes that BTES and the procedures utilized in its design and construction.

Numerous deep BHEs (DBHEs) have been developed. These include the following (sorted in chronological order):

- USA, Hawaii, 876.5 m [45,46].
- Germany, Prenzlau, 2786 m [47], still in operation with a long break, and Aachen, 2500 m [12,48].
- Switzerland, Weggis, 2281 m [49,50], and Weissbad, 1213 m [51–54].
- Poland, Sucha Beskidzka, 2864.5 m, the deepest DBHE in the world, installed in a well to a depth of 4281 m (the coaxial pipe was installed in a directional well, with a maximum deviation from the vertical of 38° [55], for research in 1999 [56]).
- China, Xi'an, eight deep borehole heat exchanger constructions with a depth between 2–2.8 km and a temperature approximately 70–90 °C [57].

There is no definition of DBHE in the literature. Multiple criteria define it, most importantly those related to drilling. Similarly, the definition of a deep borehole does not exist in the oil and gas industry. Various depths are proposed for the classification [58]. The authors propose a division based on BHE construction. Wells that are a maximum of 100 m deep, where all typical constructions (mostly U-pipes) can be installed, can be classified as shallow BHEs. The average BHE class could include BHE depths between 100 and 500 m, where the use of cement slurry as a stabilizer of diameter is required

due to hard geological conditions (loose and plastic rocks). BHEs of depths over 500 m, where only the coaxial construction is possible (for technical and economic reasons), could be classified as DBHEs.

For the current article, the primary objective was to critically review geological, construction, and other factors that affect the BHE design, including the depth, number, and distribution of the BHEs used in a system. The design of a BHE field must account for numerous technical factors affecting heat exchange performance. The proper utilization of appropriate design and analysis methods can lead to a lower number of BHEs in a field. This can save costs and permit BHE fields to be constructed in areas where the area of the field surface would otherwise be insufficient.

The research is based on thermal response test (TRT) data from BHE field A of the Laboratory of Geoenergetics, at AGH UST in Krakow, and two other BHEs. TRT data are interpreted using three methods: classical method (cm) [59], point method (pm) [60], and constant borehole resistivity method (cbm) [61].

The idea of a thermal response test was introduced by Mogensen in 1983. He suggested studying the average temperature of a borehole supplied with heat with a constant heating power. The first tests of borehole exchangers carried out in Poland and described in the literature were presented by Czekalski and Obstawski [62]. However, the first commercial test was performed and reported in 2007 [63]. Since then, newer and more accurate methods of determining the most important parameters of the so-called bottom heat source, in the form of a rock mass with BHEs, are sought after. These are:

- The effective thermal conductivity λ_{eff} of the BHE [64,65].
- The thermal resistance of the borehole R_b , [66].
- The temperature profile of the rock mass $T = f(H)$ [67,68].

Among others, Spitler and Gehlin [58], Sliwa [57], and Gonet et al. [40] have proposed methods of determining these parameters.

The thermal efficiency of a borehole heat exchanger is defined as the unitary (per one meter) heat transfer in the BHE, between the surrounding ground and the heat carrier. Therefore, the efficiency, which is the unitary BHE power, is independent of the heat flow direction, which can be either from the heat carrier to the ground in cooling mode or from the ground to the heat carrier in the heating mode of BHE operation.

Seven thermal response tests were conducted. The purpose of the research and the interpretation of its results is to determine the best well design and the most advantageous method of interpreting the test results.

The main purpose of the presented research is to compile the individual calculation results, obtained using various methods, of the most important coefficients describing borehole heat exchanger efficiency, to show the differences between them and, most importantly, to demonstrate the applicability of the constant thermal resistance method by showing slight deviations from the classical method while ignoring the impact of the thermal response test duration on the entirety of the calculations.

2. Essence of the Thermal Response Test and Research Objectives

The conducted thermal response tests (TRTs) were developed at the Laboratory of Geoenergetics, AGH University of Science and Technology in Krakow, Poland. The laboratory is equipped with its own borehole heat exchangers. Additionally, two wells are tested as a part of commercial measurements.

2.1. Theoretical Foundation of the Thermal Response Test

The partial differential form of the Fourier equation for thermal conductivity forms the basis of a TRT [69]. Such an equation allows for the determination of $T = T(r,t)$, as it describes the transient dependence of temperature T on the duration of the test t and the

distance from the heat exchanger r . The partial differential form of the Fourier equation is as follows:

$$\frac{\partial^2}{\partial r^2} + \frac{1}{r} \frac{\partial T}{\partial r} = \frac{\rho c}{\lambda} \frac{\partial T}{\partial t} \quad (1)$$

Substitution is one technique for solving such a partial differential equation. This technique transforms the partial differential Equation (1) into an ordinary differential equation. Perina [70] used this approach on the Theis equation of hydrogeology to determine the pressure distribution $p = p(r,t)$. In this technique, we let

$$u = \frac{r^2 \rho c}{4t\lambda} \quad (2)$$

and

$$\rho c = \frac{\lambda}{\alpha} \quad (3)$$

Next, we can show that

$$u = \frac{r^2}{4\alpha t} \quad (4)$$

Equation (1) then becomes:

$$\frac{\partial^2 T}{\partial r^2} + \frac{1}{r} \frac{\partial T}{\partial r} = \frac{1}{\alpha} \frac{\partial T}{\partial t} \quad (5)$$

With the substitution in Equation (4), we can write

$$T(r, t) = T_0 + \frac{q}{k\pi\lambda} \int_{\frac{r^2}{4\alpha\lambda}}^{\infty} \frac{e^{-x}}{x} dx \quad (6)$$

Through substitution of the integral in Equation (6) with a suitable expression, while recalling the substitution in Equation (4), the following is obtained:

$$T(r, t) = T_0 + \frac{q}{4\pi\lambda} \left[\ln\left(\frac{4\alpha t}{r^2}\right) - \gamma \right] \quad (7)$$

We now consider boundary and initial conditions. Note that the resulting solution is analytical rather than numerical. As an infinite linear heat source forms the TRT mathematical foundation, the differential equation is not solved over a finite region. The length of the linear source corresponds to the depth of the borehole. The duration of a TRT is set to a maximum of 100 h. The natural temperature distribution is utilized as the initial temperature distribution, following the approach of Sliwa et al. [71]. However, the temperature distribution is normally approximated as uniform at an initial temperature of T_0 . The thermal response test measures the temperature of the fluid circulating in a closed circuit of a borehole heat exchanger, through both the inlet and outlet of the exchanger. The apparatus allows for the injection of fluid at varying heating powers, volumetric flow rates, and thus at different temperatures. The entire installation is equipped with appropriate temperature and flow sensors, to monitor the behavior of the heating medium in the borehole heat exchanger at all times. The thermal response test technique is presented in Figure 1 [72].

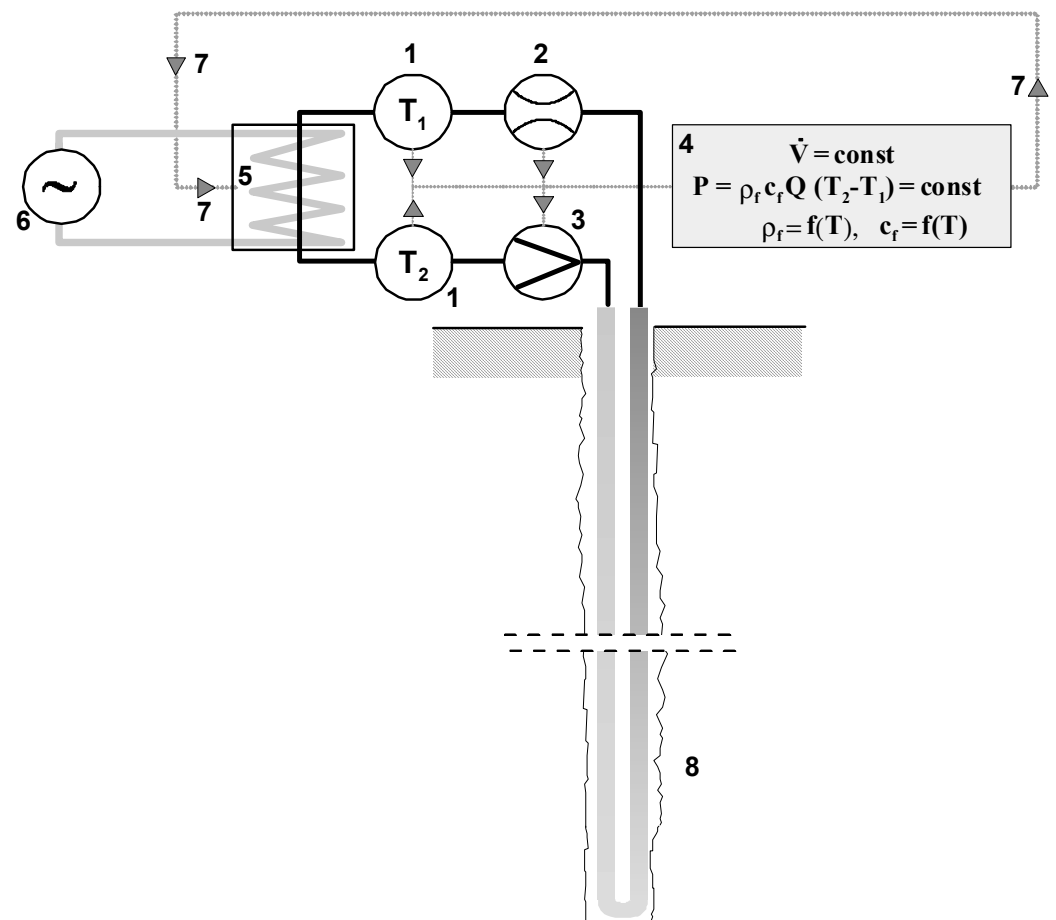


Figure 1. Schematic of thermal response test device and operation. Legend: 1 = thermometers, 2 = flow rate meter, 3 = circulating pump, 4 = control computer, 5 = heaters, 6 = electric current source, 7 = heater control signal, and 8 = BHE. In addition, the following terms are included: T = temperature, P = heat rate, \dot{V} , Q = flow rate of heat carrier, $c_f = f(T)$ = temperature-dependent specific heat of heat carrier, and $\rho_f = f(T)$ = temperature-dependent density of heat carrier.

2.2. Test Subjects

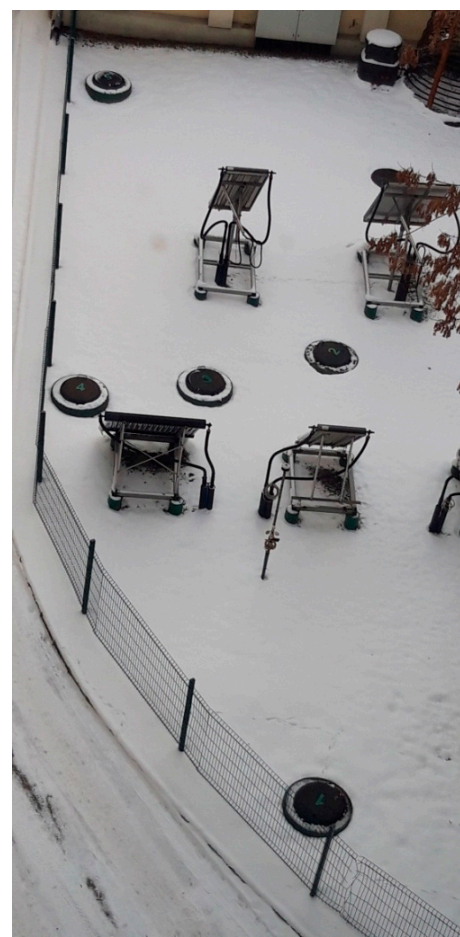
The Geoenenergetics Laboratory contains five borehole heat exchangers with varying constructions and sealing slurries, which were created between January and February 2008. The lithological profile of the tested area is shown in Table 1. The profile begins from 1.8 m because of the depth of the inspection pit (see Figure 2). The first drilled borehole heat exchanger (BHE number 3) was constructed to a depth of 84 m from the surface; however, due to the presence of underground water, a six-meter silt cork was applied. The other four boreholes (number 1–2 and 4–5) were drilled 78 m deep from the surface (76.2 m from the bottom of the inspection pit). The borehole heat exchangers (Table 2) are located in field A of the Geoenenergetics Laboratory area. According to the geological project, quaternary formations were drilled to a depth of 19.80 m with a 216 mm diameter drill bit ($8\frac{1}{2}$ "') with a mud scrubber. Casing pipes of 177.8 mm (7"') in size were used to a depth of 18.80 m in the Miocene gray clays, thus isolating the quaternary from the surface. Afterwards, the Tertiary formations were drilled by a 143 mm drill bit. In June 2008, a connection between borehole heat exchangers and cold storages was constructed [73–75]. The technical specifications of BHEs 1–5 are described in Table 2.

Table 1. Stratigraphic-lithological profile based on field A of the Geoenergetics Laboratory boreholes, with selected thermal parameters of rocks, adapted from [60].

Number	The Depth of the Layer's Top, m	The Depth of the Layer's Bottom, m	Thickness, m	Lithology	Stratigraphy	Thermal Conductivity, λ , $W \cdot m^{-1} \cdot K^{-1}$	Specific Volumetric Heat, c_v , $MJ \cdot m^{-3} \cdot K^{-1}$
1	1.8	2.2	0.4	Anthropogenic land (dark gray gully with rubble)	Quaternary (Pleistocene, Holocene)	1.600	2.000
2	2.2	2.6	0.4	Silts (gray soil)		1.600	2.200
3	2.6	4.0	1.4	Fine and dusty sand slightly muddied		1.000	2.000
4	4.0	6.0	2.0	Fine sand		1.200	2.500
5	6.0	15.0	9.0	Sandy gravel and gravel	Tertiary (Miocene)	1.800	2.400
6	15.0	30.0	15.0	Gray clay		2.200	2.300
7	30.0	78.0	48.0	Gray shale		2.100	2.300
Weighted mean						2.039	2.309



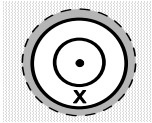
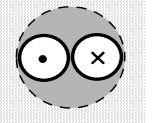
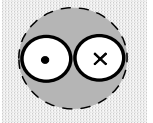
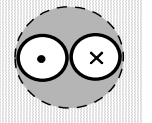
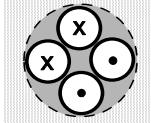
(a)



(b)

Figure 2. Inspection pits for the five borehole heat exchangers (a). Borehole heat exchangers with solar collectors for heat production and storage installed later (b). Adapted from [74].

Table 2. Constructions of borehole heat exchangers (LG-1a to LG-5a).

Parameter	LG-1a	LG-2a	LG-3a	LG-4a	LG-5a
Construction	Casing pipes PE with diameter 90 mm and wall thickness 5.4 mm, inner pipe PE with diameter 40 mm and wall thickness 2.4 mm	Single U-pipe PE with diameter 40 mm and wall thickness 2.4 mm	Single U-pipe PE with diameter 40 mm and wall thickness 2.4 mm	Single U-pipe PE with diameter 40 mm and wall thickness 2.4 mm	Double U-pipe PE with diameter 32 mm and wall thickness 2.4 mm
BHE number	1	2	3	4	5
Construction (Illustration)					
Depth of BHE, m,	76.2				
Sealing used with borehole	Cement slurry seal	Cement slurry seal	Cement slurry seal (ThermoChem) with increased thermal conductivity	Gravel on granulation between 8 and 16 mm and two clay corks—Compactonit	Cement slurry seal
Heat conductivity of fill material (hardened grout), $\lambda, \text{W}\cdot\text{m}^{-1}\cdot\text{K}^{-1}$	1.2	1.2	2.0	1.8	1.2

Boreholes F1 and F2 are in Folsz (S-Poland), and their geological profiles are described in Table 3. Borehole heat exchanger F1 (BHE number 6) has a double PE U-tube design with a nominal diameter of 32 mm and a wall thickness of 2.4 mm. Borehole heat exchanger F2 (BHE number 7) has a single PE U-tube design with a nominal diameter of 40 mm and a wall thickness of 2.4 mm. The depth of the BHEs from Folsz (number 6–7) is 100 m. In addition, these boreholes were sealed with cement slurry. The heat conductivity of the filling material is $1.2 \text{ W}\cdot\text{m}^{-1}\cdot\text{K}^{-1}$.

Table 3. Lithological profile of boreholes in Folsz, adapted from [60], Quaternary (Pleistocene, Holocene).

Number	The Depth of the Layer's Top, m	The Depth of the Layer's Bottom, m	Thickness, m	Lithology	Thermal Conductivity, $\lambda, \text{W}\cdot\text{m}^{-1}\cdot\text{K}^{-1}$	Specific Volumetric Heat, $c_v, \text{MJ}\cdot\text{m}^{-3}\cdot\text{K}^{-1}$
1	0	2.0	2.0	Sandy clay and stone gravel	1.60	2.400
2	2	7.0	5.0	Rubble stratified with clay	1.60	2.400
3	7	12.5	5.5	Shales, claystones	2.10	2.300
4	12.5	45.5	32.0	Sandstone stratified with siltstones and claystones	2.30	2.000
5	45.5	100.0	54.5	Sandy gravel and gravel	2.30	2.000
Weighted mean					2.24	2.045

3. Interpretation Methods for Thermal Response Test Results

There are three methods for determining parameters from thermal response tests. The parameters are effective thermal conductivity λ_{eff} and borehole thermal resistivity R_b . Each of the following methods was used on the same test material, i.e., the thermal response tests results, which were carried out on the wells described in Section 2.1. Knowledge of

these parameters is necessary for the proper operation of geothermal heat pumps. The classic method is currently in use.

3.1. Classic Method (cm) of Determining Parameters from Thermal Response Tests

The slope methodology is the most basic and common methodology for the underground thermal conductivity from a TRT [57,76]. The mean temperature is plotted against the logarithm of time. The slope of the curve thus represents the thermal. This expression is derived from the common expression for infinite line supply. Under the assumption that the heat is discharged from the borehole, where it depends solely on radial conduction, which for the time scale of a TRT is a valid approximation, the mean fluid temperature can be written as Equation (7) [60] and the heat losses per unit depth q as:

$$q = \frac{P}{H} \tag{8}$$

The time of the test and the time assumed as the beginning of interpretation of the above function in the semilogarithmic system are important in each TRT. It was determined that, according to Equation (10), the calculation error is 2.5% when the time is longer or equal to $20 \cdot r_b^2 \cdot \alpha^{-1}$ and 10% when $t \geq 5 \cdot r_b^2 \cdot \alpha^{-1}$. In many TRT interpretations, the temperature is determined at the inlet and outlet of the heat carrier as a function of the test duration time [39].

Pursuant to the measurement of the supply and return temperature of the heat carrier, it is possible to determine the relationship between the average temperature T_f and the test duration t [77]. Creating a chart of interdependence between the average temperature of the fluid T_f and the logarithm of the test duration $\ln(t)$ is a good method of evaluation of thermal response test data.

The chart has a linear character with regards to $\ln(t)$. The slope of the k curve allows for the assessment of effective thermal conductivity λ_{eff} equations, as follows:

$$\lambda_{eff} = \frac{P}{4 \cdot \pi \cdot H \cdot k} \tag{9}$$

where

$$P = \frac{\sum_{i=1}^n P_{chi}}{n} \tag{10}$$

$$P_{chi} = \dot{V}_i \cdot c_i \cdot \rho_i \cdot \Delta T_i \tag{11}$$

Another important BHE parameter is its thermal resistivity R_b , defined as:

$$R_b = \frac{1}{q} (T_{av} - T_0) - \frac{1}{4 \cdot \pi \cdot \lambda} \left[\ln \left(\frac{4\alpha t}{r_b^2} \right) + \frac{r_b^2}{4\alpha t} - \gamma \right] \tag{12}$$

where

$$T_{av} = \frac{T_f + T_r}{2} \tag{13}$$

With the proper parameters, it is possible to achieve a good characteristic of the ground source heat pump, that is, a high coefficient of performance (COP) value.

3.2. Point Method (pm) of Determining Parameters from Thermal Response Tests

The effective thermal conductivity coefficient of the borehole R_b can also be calculated as [60]:

$$\lambda_{eff} = \frac{q}{4\pi} \frac{\left[\ln \left(\frac{t_2}{t_1} \right) + \frac{r_b^2(t_2 - t_1)}{4 \cdot \alpha \cdot t_1 \cdot t_2} \right]}{T(t_2) - T(t_1)} \tag{14}$$

Times t_1 and t_2 refer to the beginning and the end of the range for which the λ_{eff} coefficient is calculated. The temperatures $T(t_1)$ and $T(t_2)$ are read from the linear regression function for the average temperature of the heat carrier, calculated as:

$$T_{av} = \frac{T_{in} + T_{out}}{2} \quad (15)$$

The temperatures $T(t_1)$ and $T(t_2)$ are determined as follows:

- Having the following data: $\ln(t_1)$ or $\ln(t_2)$ and T_{av} , the slope coefficient k and the intersection point of the line with the vertical axis (point b) are determined for a given time range. The intersection point is the point where the regression line, taken through known values $\ln(t_1)$ or $\ln(t_2)$ and T_{av} , intersects the vertical axis. That is,

$$b = \overline{T_{av}} - k \cdot \ln(\overline{t_1}) \quad \text{or} \quad b = \overline{T_{av}} - k \cdot \ln(\overline{t_2}) \quad (16)$$

- Then, the following equation can be written:

$$T_{av(reg)} = k \cdot \ln(t_1) + b \quad \text{or} \quad T_{av(reg)} = k \cdot \ln(t_2) + b \quad (17)$$

With this approach, the influence of possible disturbances on the registration of temperatures during the thermal response test at the boundaries of the tested period (t_1 and t_2) in Equation (17) is avoided. Then, the borehole thermal resistance R_b is calculated with Equation (15).

3.3. Constant Borehole Resistivity Method (cbm) of Determining Parameters from Thermal Response Tests

Unfortunately, the fact is that an almost ideal thermal response test run does not always guarantee similar results for the effective thermal conductivity λ_{eff} and thermal resistivity of the borehole, as demonstrated with the data evaluated by Sliwa [61] and checked by Sapińska-Śliwa [78]. This is due to differences between analyzed data. In many cases, it is possible to observe that the thermal conductivity value varies with the TRT duration. Therefore, a new method of determining parameters from a thermal response test, where data are not significantly affected by the test duration, is proposed. Figure 3 illustrates the relationship between thermal resistivity R_b and the duration of thermal response test t . The only difference between the graphs is the thermal conductivity λ in Equation (12) [60].

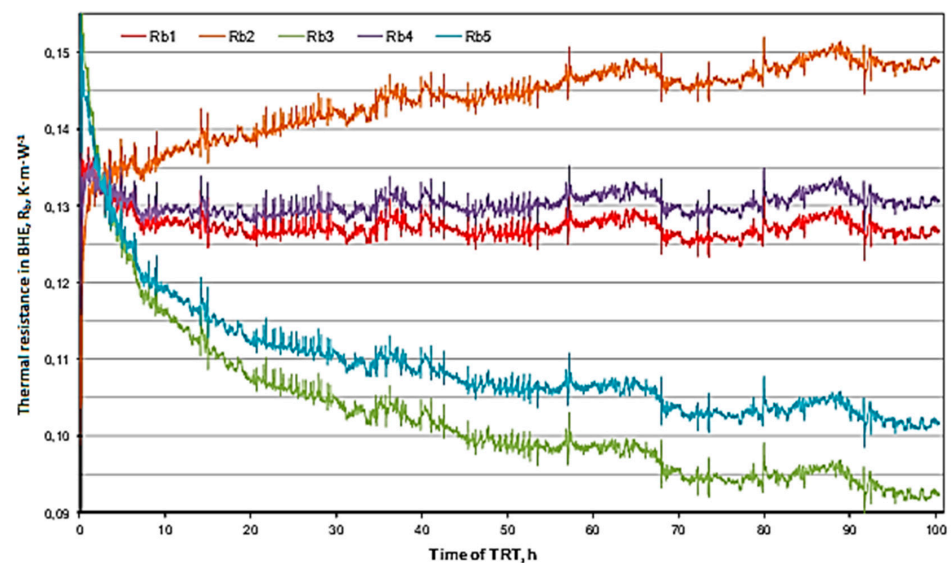


Figure 3. Thermal resistivity of BHE vs. TRT time, where R_{b1} , R_{b2} , R_{b3} , R_{b4} , and R_{b5} are values for different thermal conductivities given in Equation (12).

The new solution, proposed by Sliwa (2012), is to determine the value of λ_{eff} such that the linear regression based on experimental relation $R_b = f(t)$ takes the form of the function $R_b = kt + b$, where the slope coefficient of the straight trend line, representing the heat carrier temperature graph as a function of the natural logarithm of the TRT heating time k , is equal (or close) to zero [61]. Determining the values of λ_{eff} and R_b comes down to finding λ_{eff} , where $k = 0$. Then, we evaluate $R_b = b$ [60]. This can be described based on (15) as:

$$R_b(t) = kt + b \quad (18)$$

$$R_b(t) = \frac{1}{q}(T_{av} - T_0) - \frac{1}{4 \cdot \pi \cdot \lambda_{eff}} \left[\ln \left(\frac{4\alpha t}{r_b^2} \right) + \frac{r_b^2}{4\alpha t} - \gamma \right] = b \quad (19)$$

$$b = \frac{1}{q}(T_{av} - T_0) \quad (20)$$

$$-k \frac{H}{P} \left[\ln \left(\frac{4\alpha t}{r_b^2} \right) + \frac{r_b^2}{4\alpha t} - \gamma \right] = 0 \quad (21)$$

$$k = 0 \quad \text{when } \lambda = \lambda_{eff} \quad (22)$$

4. Test Results

The results from the thermal response test are as follows:

- The time from the onset of heating, s.
- The fluid temperature inlet to the exchanger, °C.
- The fluid temperature returning from the exchanger, °C.
- The outside (atmospheric) temperature, °C.
- The temporary flow rate, dm³/min.

The borehole diameter is $d = 0.143$ m for all heat exchangers. Note that the set temperature of the profile can be determined by recording the temperature of the medium circulating inside the borehole heat exchanger before the heating process. The value of this temperature can be determined by temperature profiling. In the case of heat exchangers at the AGH University of Science and Technology (1, 2, 3, 4, 5) and Folsz (6, 7), the established temperature of the profile T_0 was previously designated by the NIMO-T probe. If heat power P and depth of exchanger H are known, it is possible to calculate the unit heat power q . The obtained results of temperature, depth, and unit heating power (the heating power for every BHE was 4 kW) of each exchanger are presented in Table 4.

Table 4. Values of the set average temperature of the profile T_0 , depth of exchangers H , and unit heating power q .

BHE Number	1	2	3	4	5	6	7
$T_0, ^\circ\text{C}$	12.68	12.73	12.72	13.18	12.71	10.17	10.33
H, m			76.2			100.0	
$q, \text{W} \cdot \text{m}^{-1}$			52.36			40.00	

Graphs of the relationship between the fluid's initial and return temperatures, as well as its heating time, were created from the results of the thermal response test carried out on each borehole heat exchanger. This method shows how the temperature of the medium flowing through the heat exchanger varies over time. Based on studies of Grygieńcza in 2009 [79], a comparison was made, as shown in Figures 4–10. The duration of the heating phase of each thermal response test was not strictly identical; however, it did not affect further calculations (it was always over 70 h).

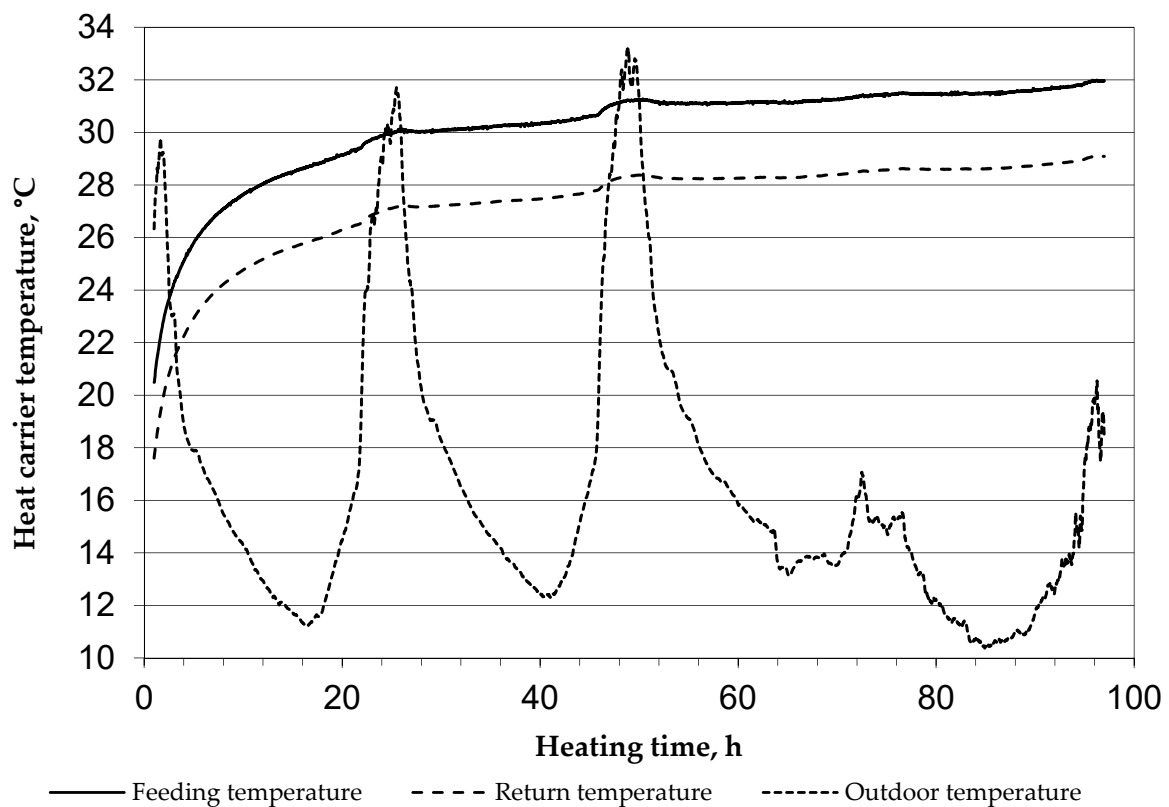


Figure 4. Relationship between heat carrier temperature and heating time in BHE LG-1a (coaxial construction).

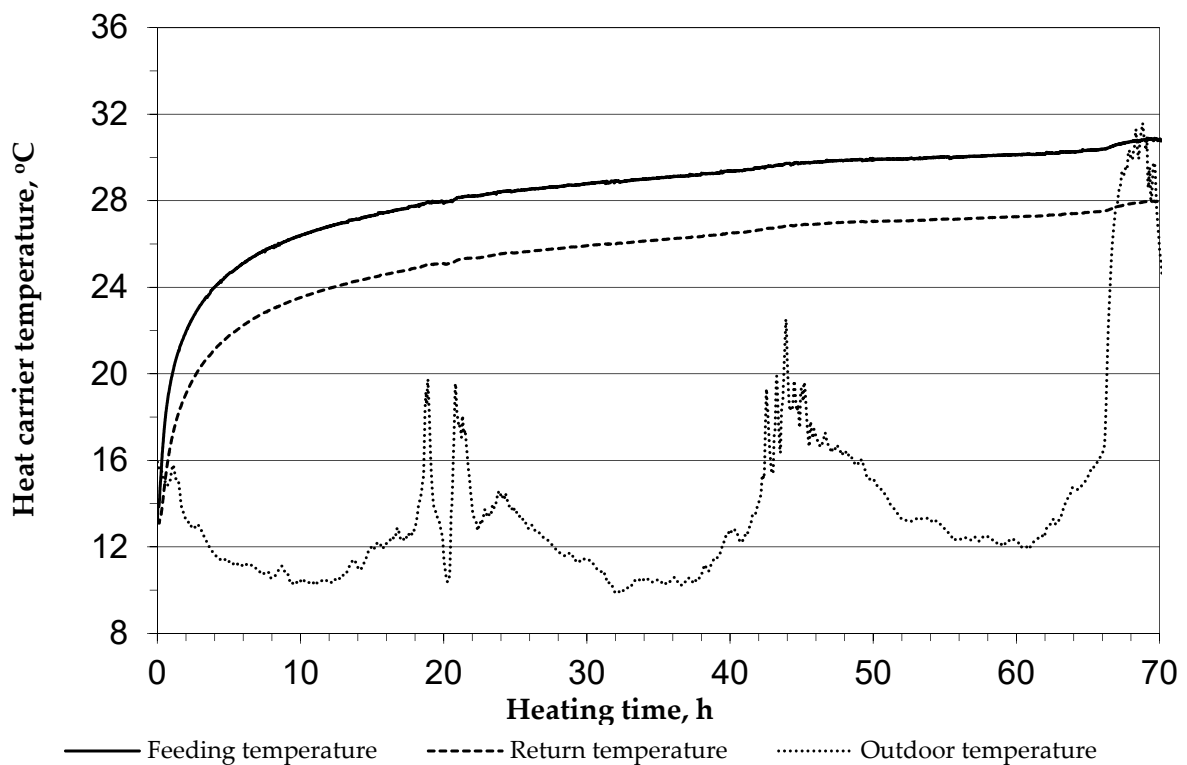


Figure 5. Relationship between heat carrier temperature and heating time in BHE LG-2a (single U-pipe with cement slurry seal).

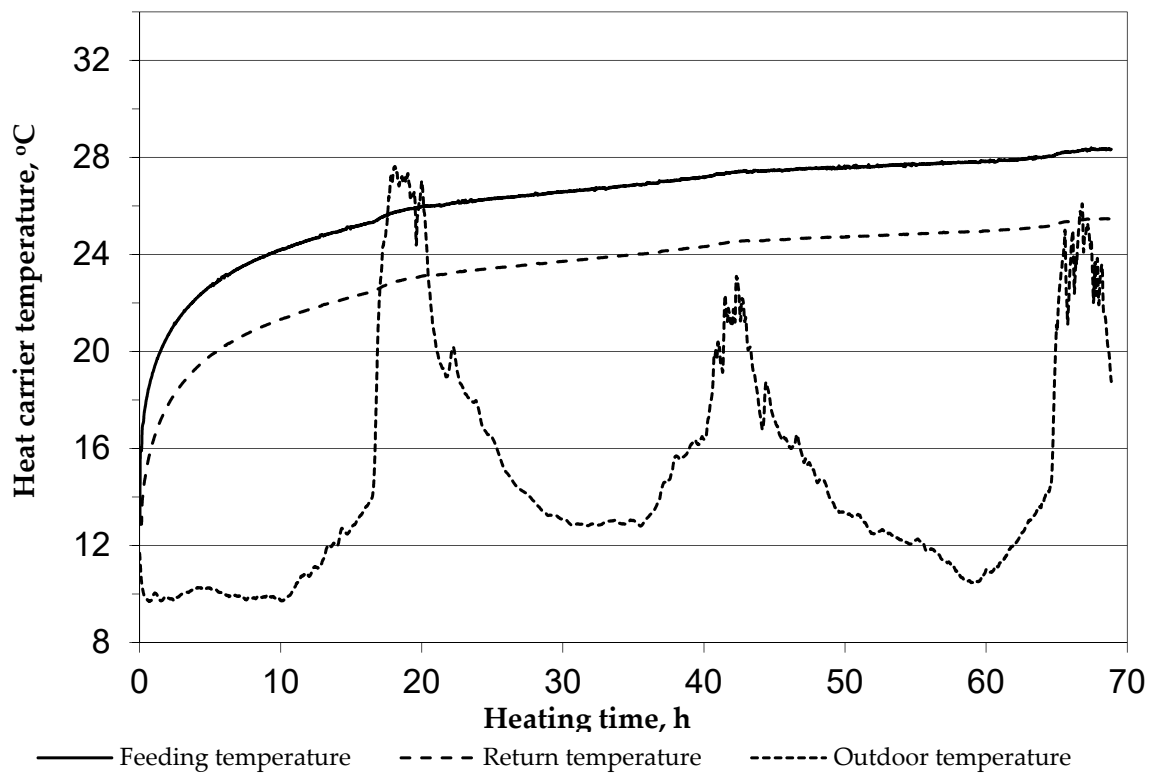


Figure 6. Relationship between heat carrier temperature and heating time in BHE LG-3a (single U-pipe with slurry seal with increased thermal conductivity).

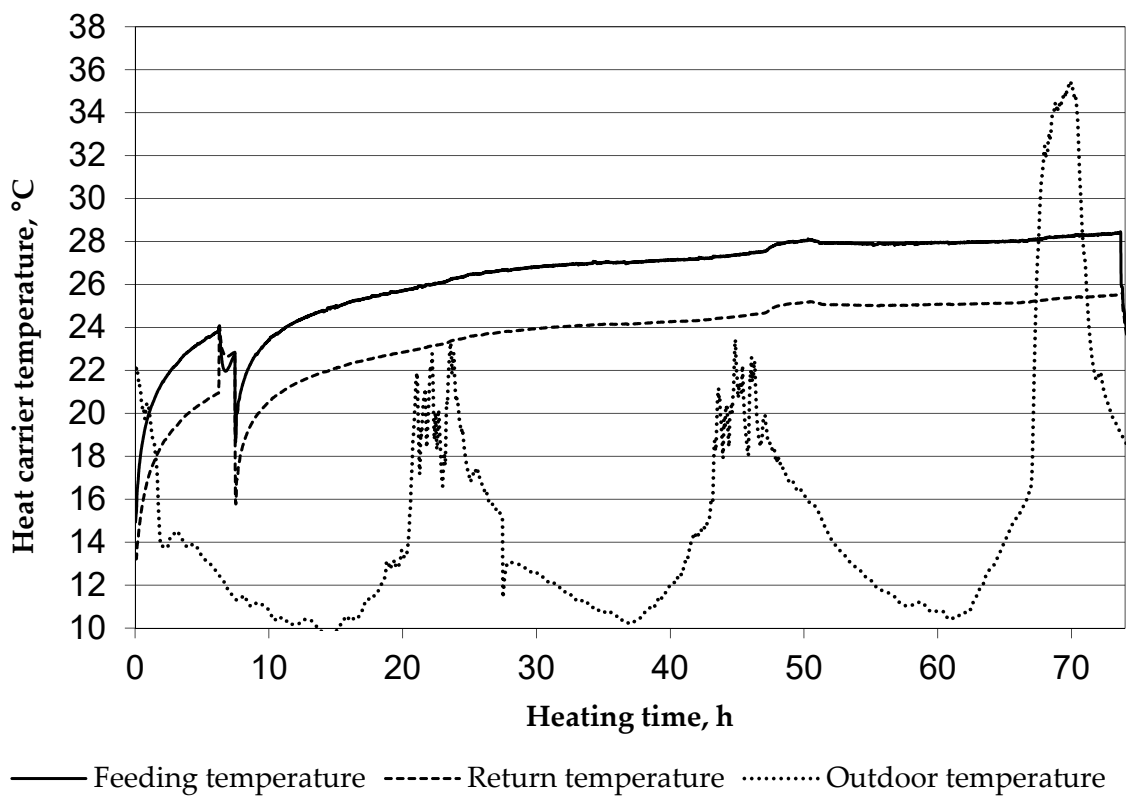


Figure 7. Relationship between heat carrier temperature and heating time in BHE LG-4a (single U-pipe with gravel).

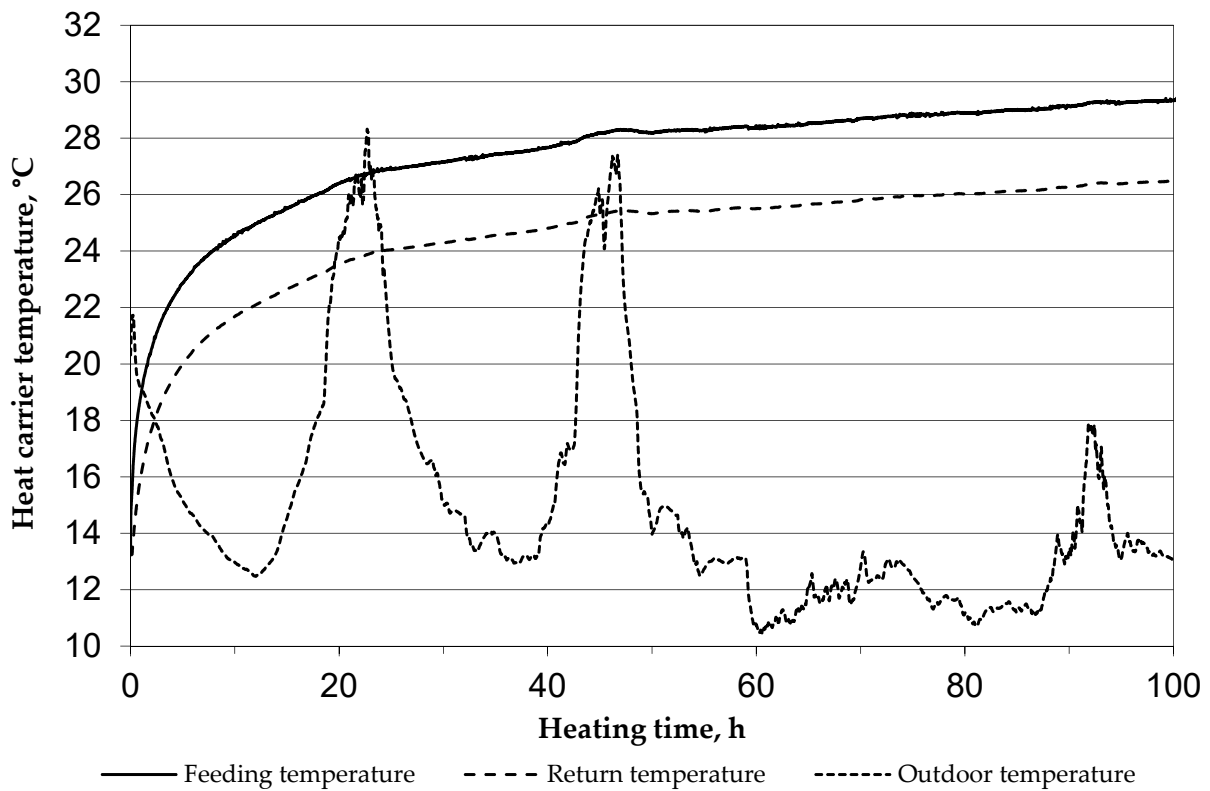


Figure 8. Relationship between heat carrier temperature and heating time in BHE LG-5a (double U-pipe).

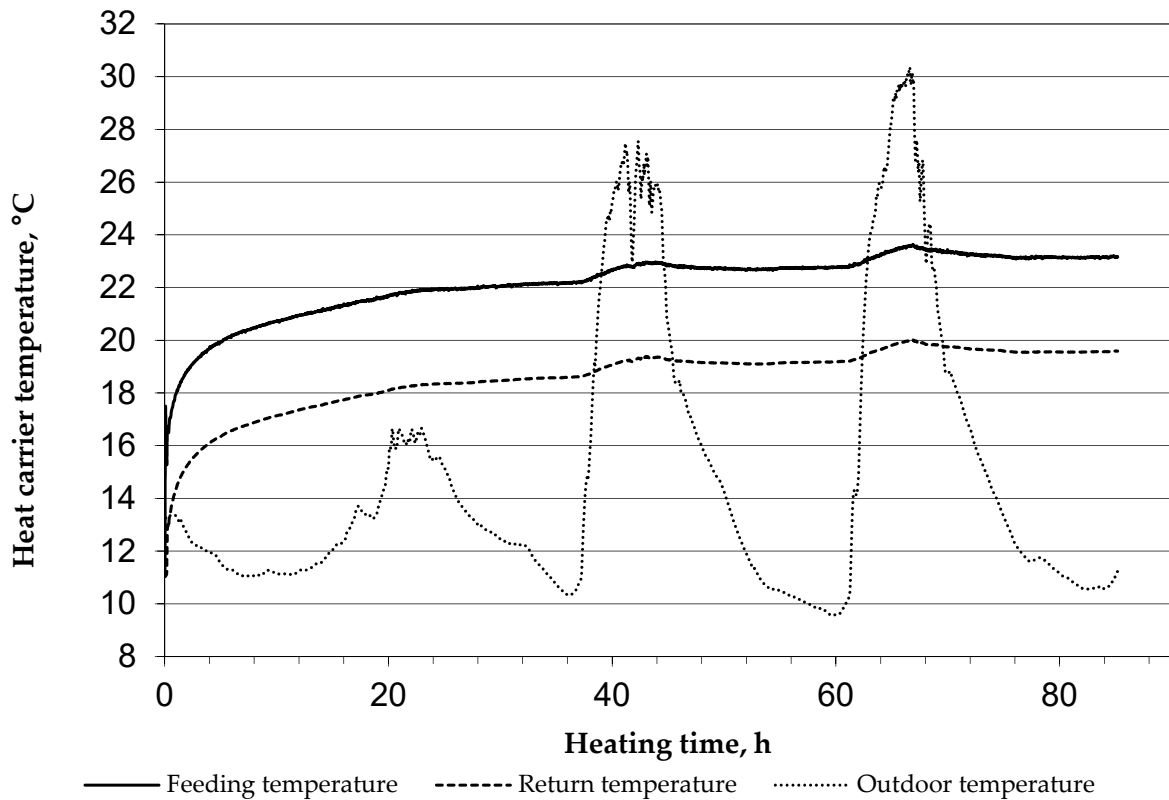


Figure 9. Relationship between heat carrier temperature and heating time in BHE F1 (double U-pipe).

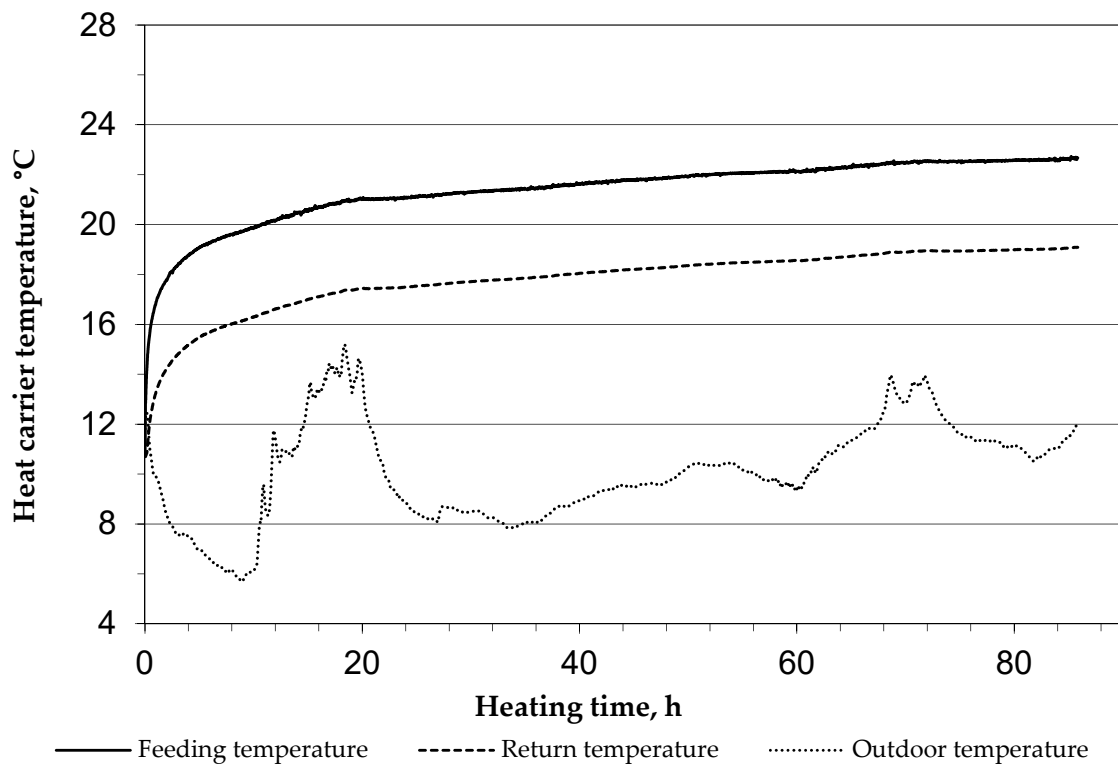


Figure 10. Relationship between heat carrier temperature and heating time in BHE F2 (single U-pipe).

The heat carrier temperature values in Figures 4–10 during the 70th hour of each test are listed and compared in Table 5. The highest temperature was achieved in the centric design well (LG-1a), while a slightly lower temperature was observed in well LG-2s. Very similar temperatures were exhibited in wells 3–5. As presented in the last column, the temperature difference values are similar for all wells in the Laboratory of Geoenergetics. This is due to the almost identical value of the heat carrier flux. However, the values for the wells in Folsuz are different. Despite the identical heat carrier flux, the carrier temperature is lower and the temperature difference is higher. This is reflected in the fact that the heat-dissipating medium, i.e., the rock mass, has a higher thermal conductivity. Due to the greater conductivity of the rocks and the faster heat dissipation, the inflow and outflow temperatures are lower in the Folsuz wells.

Table 5. Summary of heat carrier temperature values in the 70th hour of the thermal response test.

BHE NUMBER	BHE NAME	INFLOW TEMPERATURE, °C	OUTFLOW TEMPERATURE, °C	AVERAGE FLOW TEMPERATURE, °C	HEAT CARRIER VOLUMETRIC FLOW RATE, DM ³ /MIN	TEMPERATURE DIFFERENCE (INFLOW TO OUTFLOW), °C
1	LG-1a	31.261	28.394	29.828	20.00	2.867
2	LG-2a	30.848	27.941	29.395	19.99	2.907
3	LG-3a	28.336	25.462	26.899	20.00	2.874
4	LG-4a	28.044	25.168	26.606	19.89	2.876
5	LG-5a	28.704	25.824	27.264	20.00	2.880
6	F1	23.392	19.749	21.571	20.00	3.643
7	F2	22.486	18.899	20.693	20.00	3.587

The atmospheric air temperatures measured during the tests allow for the evaluation of their influence on the tests. It is seen that increases in air temperature during the day have a minimal effect on the behavior of the two measured temperatures of the heat carrier. Therefore, this influence was ignored in calculations.

Figures 11–17 illustrate a relationship between the average heat carrier temperature and the logarithm of the TRT time (curve) and simple regression (thin dashed line). The need for creating these charts is explained in detail in Section 3.1 (classic method).

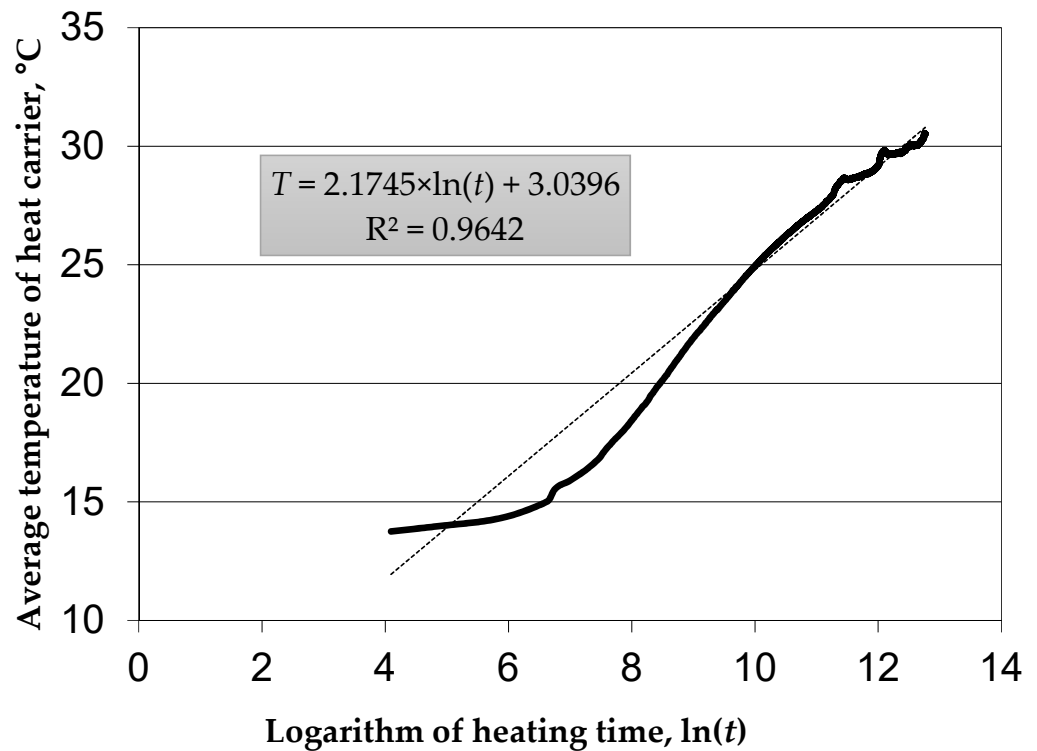


Figure 11. Relationship between average heat carrier temperature and the logarithm of heating time in BHE LG-1a (coaxial).

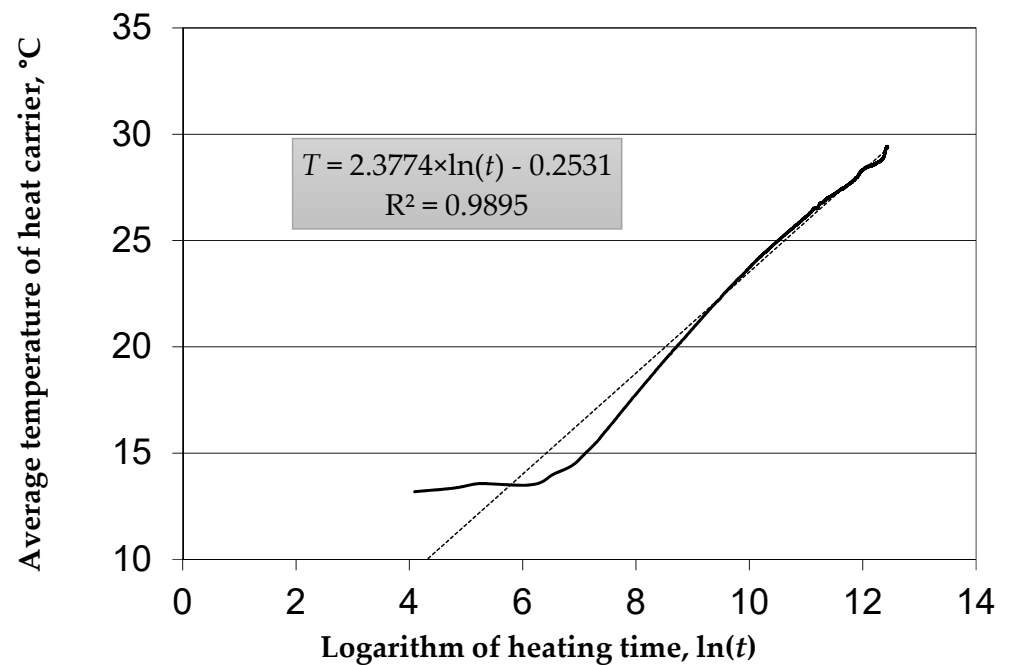


Figure 12. Relationship between average heating medium temperature and the logarithm of heating time in BHE LG-2a (single U-pipe with cement slurry seal).

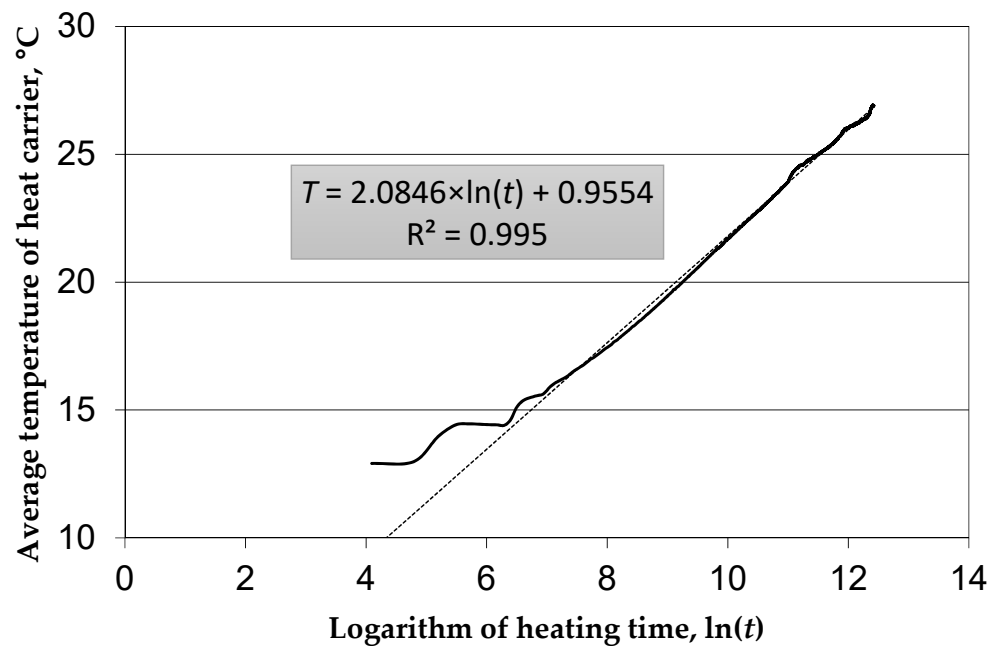


Figure 13. Relationship between average heating medium temperature and the logarithm of heating time in BHE LG-3a (single U-pipe with slurry seal with increased thermal conductivity).

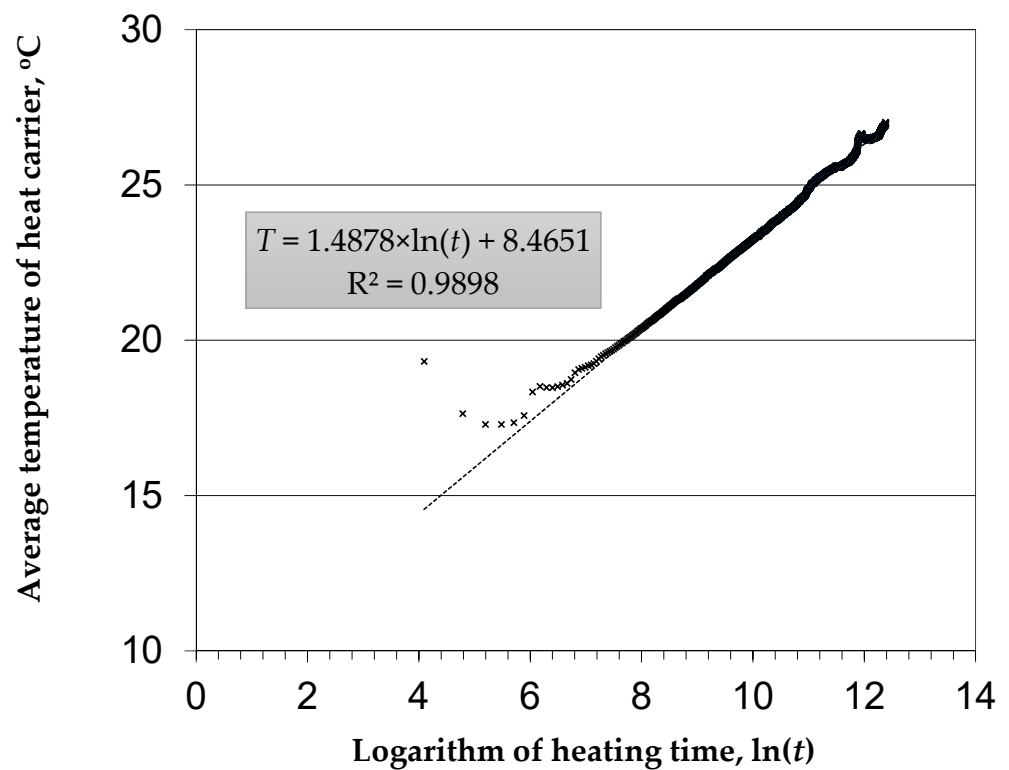


Figure 14. Relationship between average heating medium temperature and the logarithm of heating time in BHE LG-4a (single U-pipe with gravel).

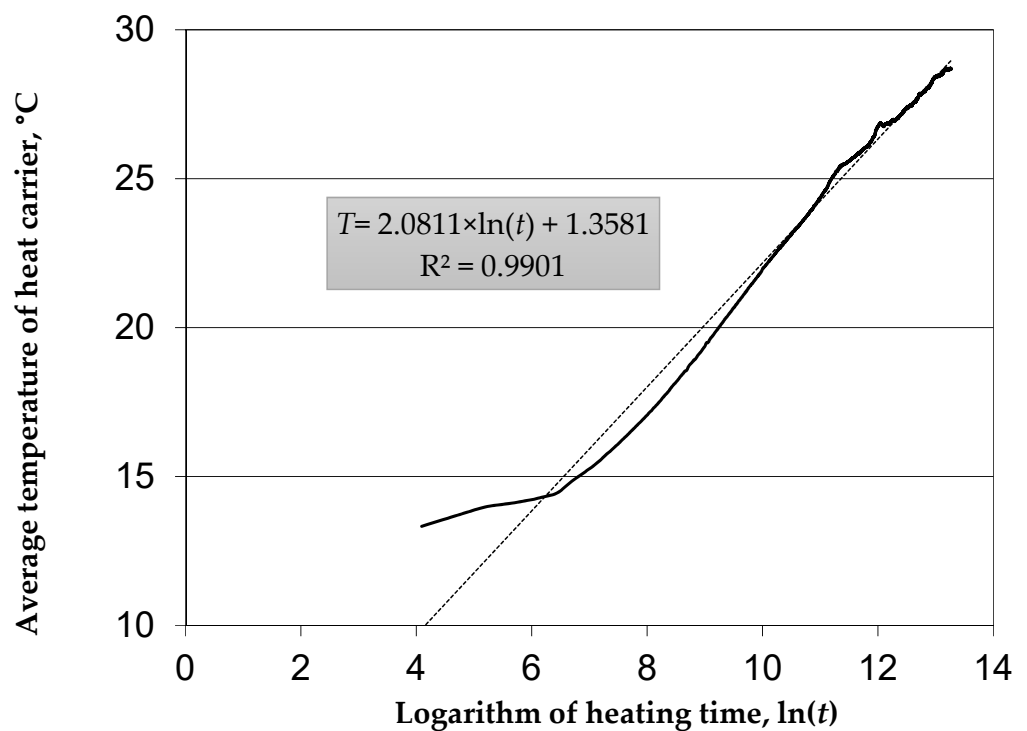


Figure 15. Relationship between average heating medium temperature and the logarithm of heating time in BHE LG-5a (double U-pipe).

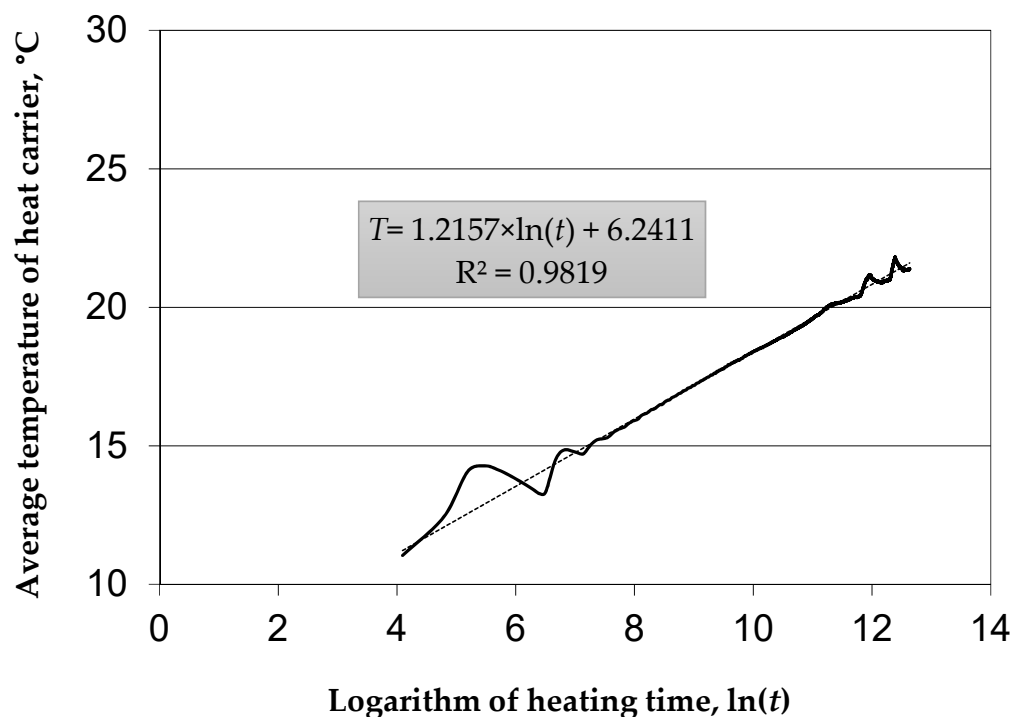


Figure 16. Relationship between average heating medium temperature and the logarithm of heating time in BHE F1 (double U-pipe).

The results shown in Figures 11–17 demonstrate the quality of the tests. Good fits are obtained using a regression line. The weakest in terms of quality was the test of the LG-1a well, where a comparatively high correlation coefficient of 0.9642 was obtained.

Note that each data set in Figures 11–17 includes values recorded every 60 s. Thus, for the 100 h test, 6000 measurement points are registered.

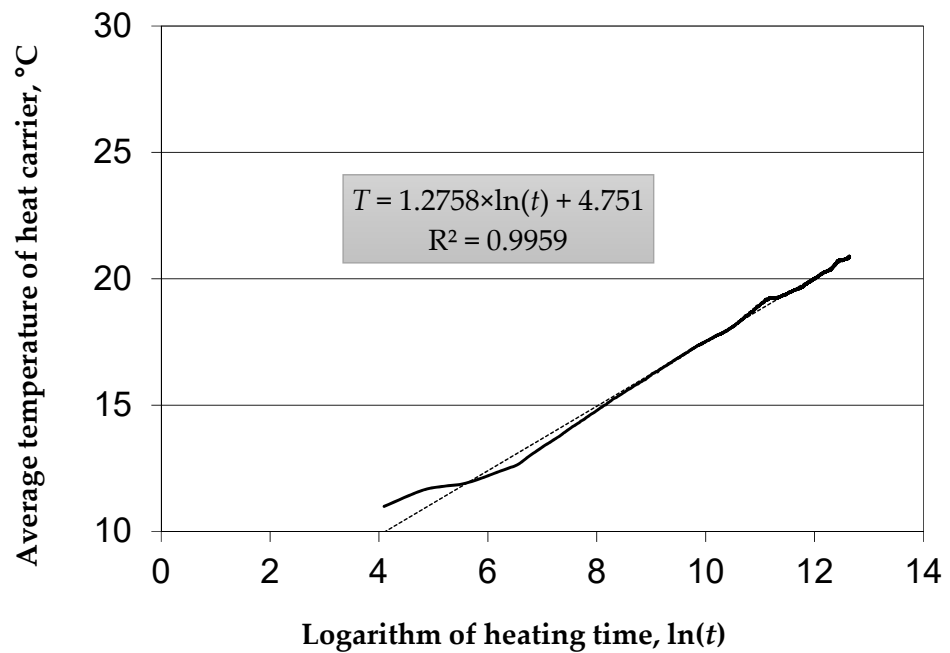


Figure 17. Relationship between average heating medium temperature and the logarithm of heating time in BHE F2 (single U-pipe).

Analysis of the TRT Results

Figures 18–25 plot the relationship between the thermal resistance R_b and test duration for the borehole heat exchangers. Note that the linear regression curve is almost horizontal to the x -axis. This is the characteristic curve appearance for the new method of analyzing data from thermal response tests, where k is close to zero. In such a case, the value of the correlation coefficient R^2 is also close to zero.

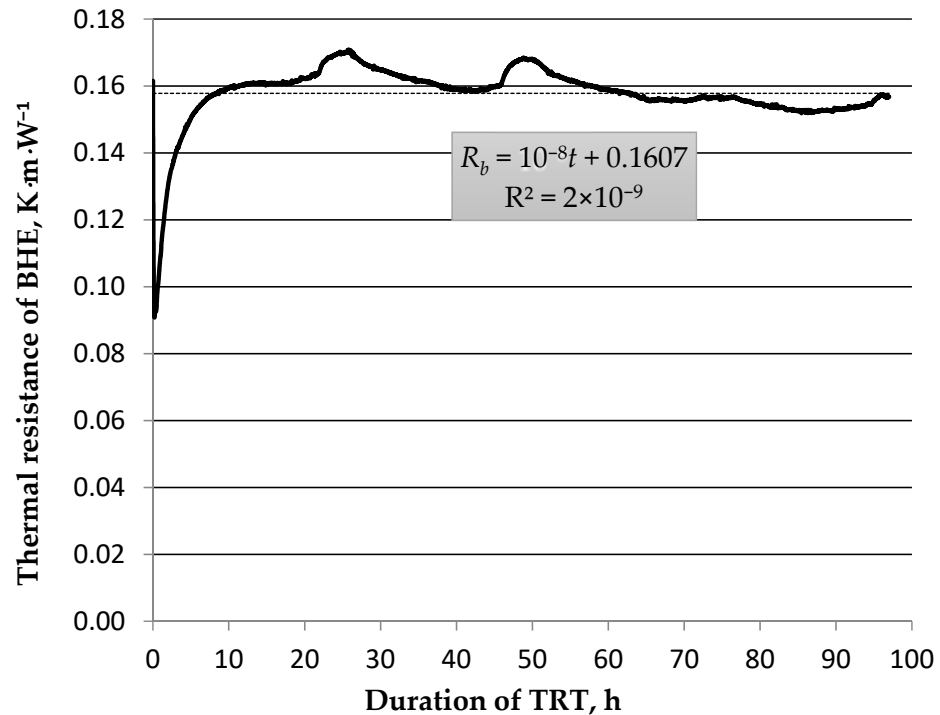


Figure 18. Relationship between thermal resistance of BHE and duration of the TRT in BHE LG-1a (coaxial).

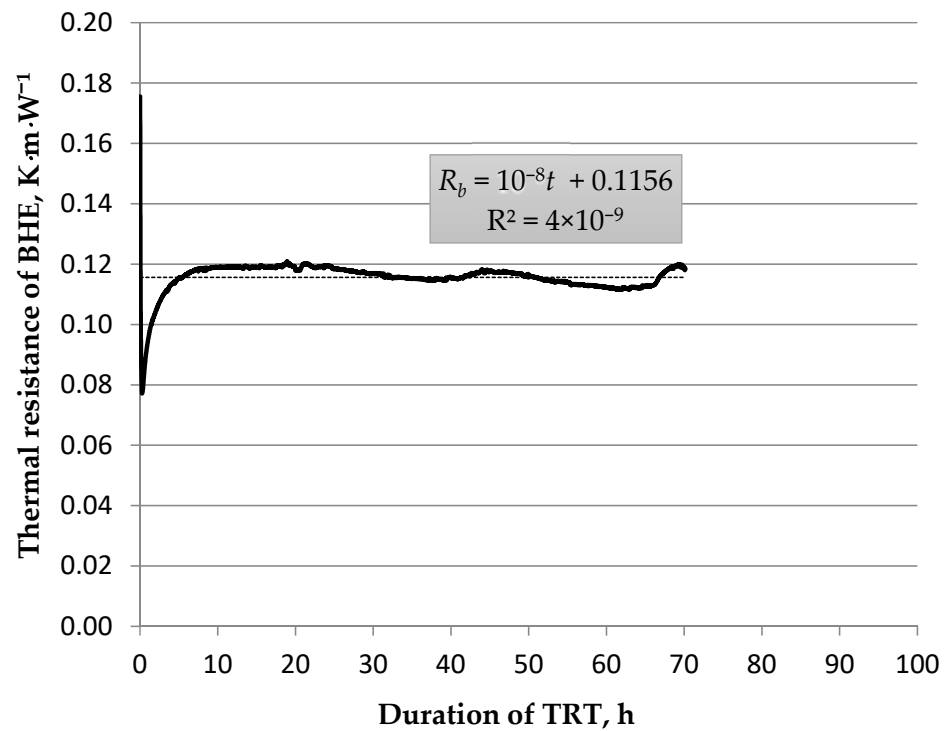


Figure 19. Relationship between thermal resistance of BHE and duration of the TRT in BHE LG-2a (single U-pipe with cement slurry seal).

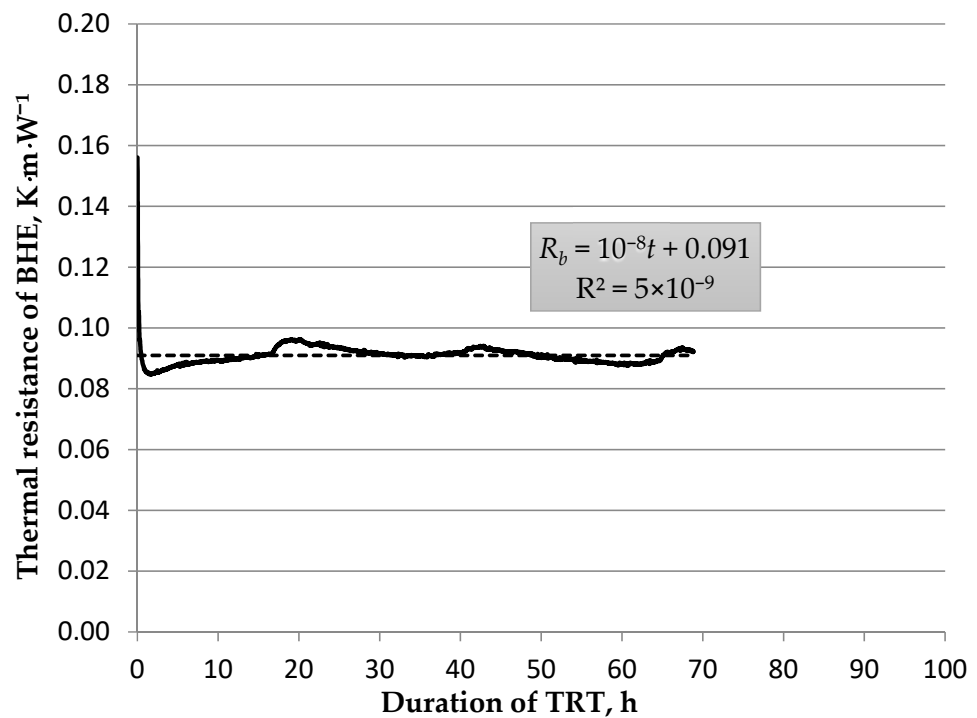


Figure 20. Relationship between thermal resistance of BHE and duration of the TRT in BHE LG-3a (single U-pipe with slurry seal with increased thermal conductivity).

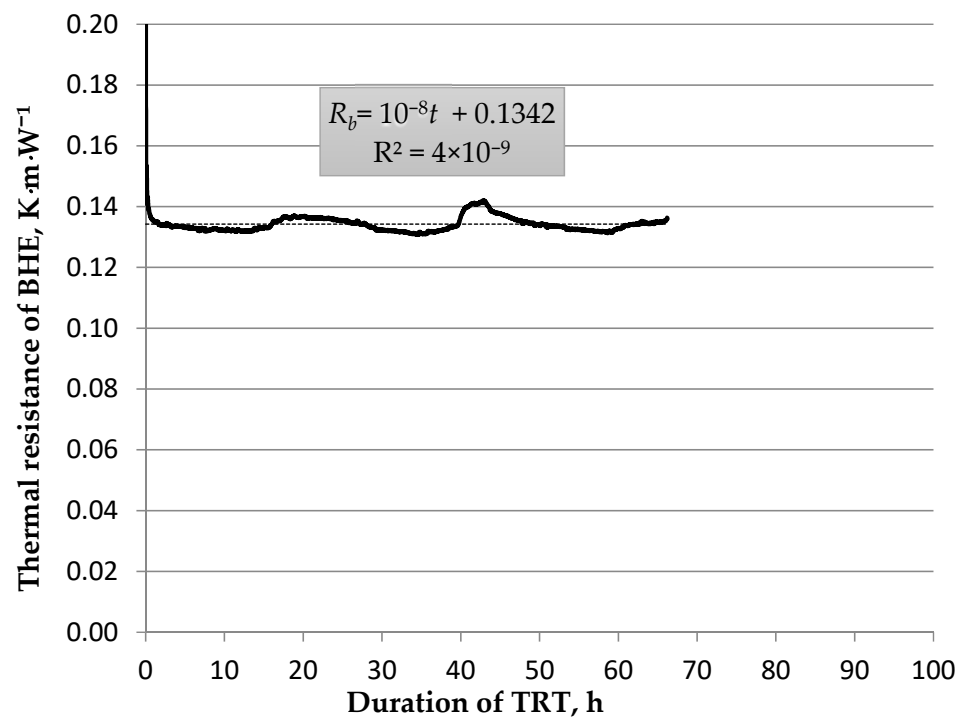


Figure 21. Relationship between thermal resistance of BHE and duration of the TRT in BHE LG-4a (single U-pipe with gravel).

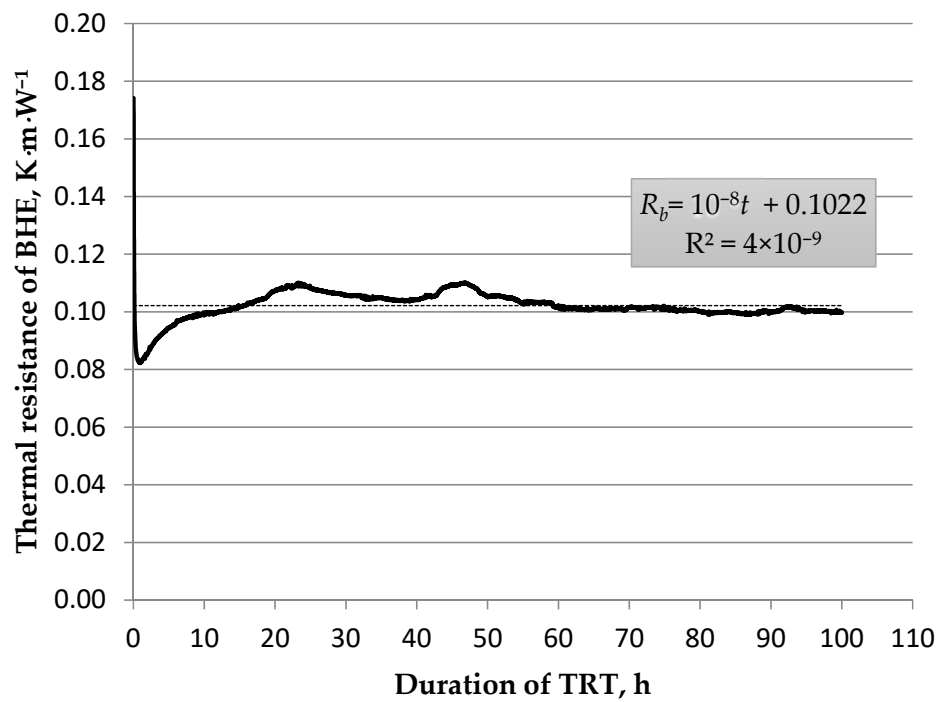


Figure 22. Relationship between thermal resistance of BHE and duration of the TRT in BHE LG-5a (double U-pipe).

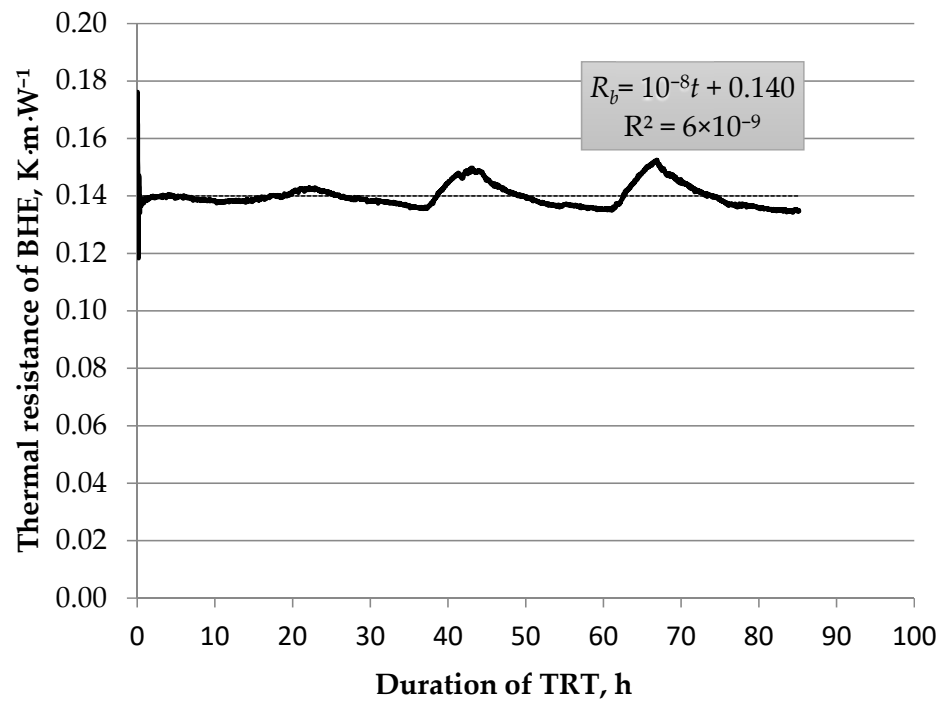


Figure 23. Relationship between thermal resistance of BHE and duration of the TRT in BHE F1 (double U-pipe).

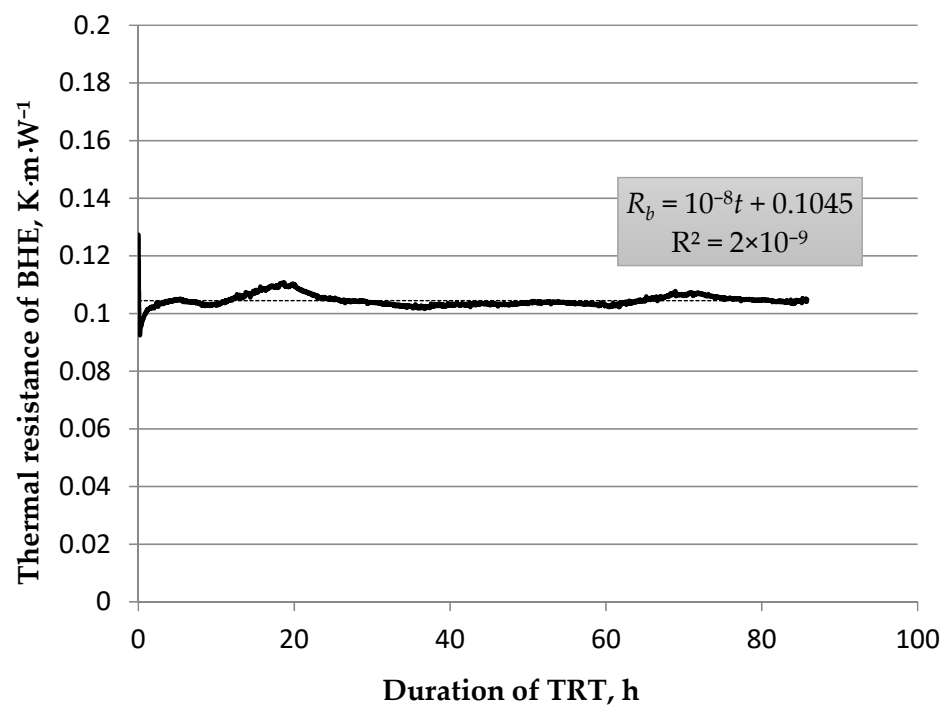


Figure 24. Relationship between thermal resistance of BHE and duration of the TRT in BHE F2 (single U-pipe).

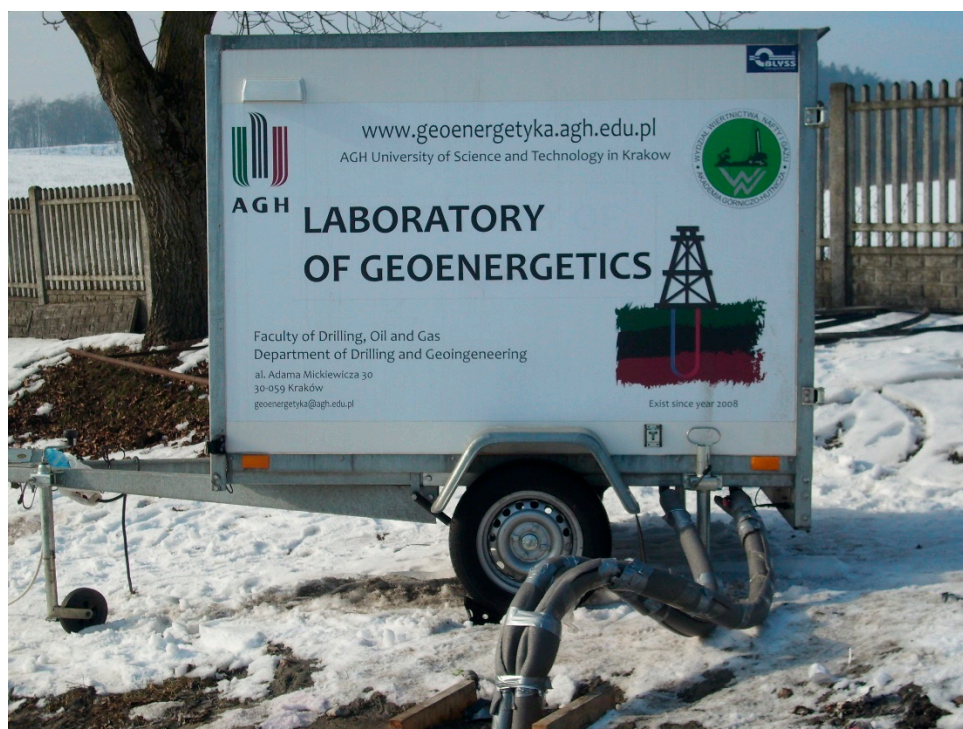


Figure 25. Thermal response test equipment of the Laboratory of Geoenergetics, AGH University of Science and Technology, Poland.

The graphs in Figures 18–25 all have very small correlation coefficients. This indicates a lack of correlation and corresponds to a linear constant function. There are clear differences in the values indicated on the vertical axes representing the thermal resistance value of the borehole heat exchangers for the different cases considered.

The tests were performed using measuring and recording equipment. The measuring equipment is from the Laboratory of Geoenergetics, AGH University of Science and Technology, and is shown in Figure 25. The apparatus is very accurate and sensitive to many variables affecting the research. For example, the constant heating power stabilization algorithm takes into account the relationship between the density and specific heat of the heat carrier and its temperature, which is variable during BHE testing.

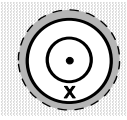
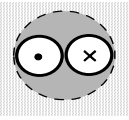
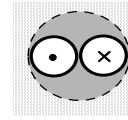
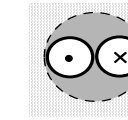
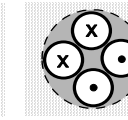
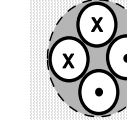
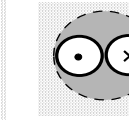
5. Data Interpretation and Results

The values obtained using the old (classic) method of analysis were compared with the values obtained using the new method in Table 6. The value calculated with the classic method indicates a very low thermal resistance coefficient, and the discrepancies may be due to the imperfection of the measurement method itself and errors in the temperature reading during the thermal response test. The most important factor is the BHE construction. There are various possibilities for problems in construction, such as quality of grout filling and distance between pipes forming a U-pipe. Measuring them is not possible. One way to determine the necessary values is to carry out testing of a large number of different BHEs in the same geology and using statistical approaches.

The standard deviation for thermal conductivity (λ) was calculated to illustrate the extent to which the results differ for the thermal conductivity calculated by each of the three methods.

The standard deviation for the thermal resistance (R_b) was calculated in the same way as for the thermal conductivity. The results of using each of the three methods were compared to check the deviation of the results.

Table 6. Results comparison.

BHE Number	1	2	3	4	5	6	7	Number of Max/Min Values
BHE Name	LG-1a	LG-2a	LG-3a	LG-4a	LG-5a	F1	F2	
BHE Construction								
	Coaxial	Single U-Pipe + Cement	Single U-Pipe + Thermal Cement	Single U-Pipe + Gravel	Double U-Pipe	Double U-Pipe	Single U-Pipe	
k	2.1745	2377	2.085	1.488	2.081	1.216	1.276	-
λ_{cm}	1.917	1.753	2.003	2.802 ↑	1.962	2.701	2.600	1
λ_{cbrm}	2.121 ↑	1.829 ↑	1.981	2.716	1.980	2.724	2.617	2
λ_{pm}	1.905	2.403	2.072 ↑	2.075	1.980	2.802 ↑	2.910 ↑	3
λ_{avr}	1.981	1.995	2.019	2.531	1.974	2.742	2709	-
Standard deviation	0.121	0.355	<u>0.047</u>	0.397	0.000	0.053	0.174	-
$R_{b,cm}$	0.151	0.151	0.124	0.045 ↓	0.135	0.125 ↓	0.112	2
$R_{b,cbrm}$	0.161	0.116 ↓	0.091 ↓	0.134	0.102	0.140	0.104 ↓	3
$R_{b,pm}$	0.138 ↓	0.147	0.093	0.097	0.099 ↓	0.141	0.113	2
$R_{b,avr}$	0.150	0.138	0.103	0.092	0.112	0.135	0.110	-
Standard deviation	<u>0.012</u>	0.019	0.019	0.045	0.020	0.009	0.005	-

The values calculated using the old method are marked with the subscript *cm* (classic method), and the values calculated using new methods are marked with the subscript *cbrm* (constant borehole resistivity method) and *pm* (point method).

In Table 6, the worst results for each method are marked in italics and the best results in bold. As can be seen from the values of standard deviations, the results are to varying degrees spread out. Symbol ↑ denotes the highest value of λ_{eff} for a given well amongst the three methods and symbol ↓ the lowest value of R_b . Note that the development of methods and models for calculating the values of λ_{eff} and R_b based on the interpretation of numerically modelled thermal response tests is the subject of planned future work by the authors.

The best borehole is seen to be a system with a single U-tube, according to the highest effective thermal conductivity λ_{eff} criterion and the lowest thermal resistance R_b criterion. The weakest BHE case according to the λ_{eff} criterion is the double U-pipe, while according to the R_b criterion it is a coaxial design. This last result is surprising but possible, e.g., when the space between the outer pipe and the borehole wall is poorly filled.

When analyzing the research in terms of the interpretative method used, no entirely unambiguous evaluations were obtained. For λ_{eff} , the highest number of maximum values (3) was obtained for the point method. For R_b , the highest number of minimum values was obtained (3) for the constant borehole resistivity method. The use of the three interpretation methods for the evaluation of the quality of the TRT results will be further investigated in the future. Further tests on new wells (BHEs) will be performed. The TRT results obtained from the mathematical modeling of the tests will also be interpreted. In subsequent reports by the authors about the effectiveness of the three-method interpretation for the evaluation of test quality, the results of new studies will be described. The aim of the new interpretation for new TRTs will be the key focus for this work rather than BHE comparisons.

6. Conclusions

In the present research, results are obtained using various methods of the most important coefficients describing borehole heat exchanger efficiency, illustrating differences and demonstrating the applicability of the constant thermal resistance method relative to the classical method. Several conclusions can be drawn from the results of the research:

- The measurements were conducted for two locations, i.e., for two different geological profiles, and thus are limited. For a more robust and broad analysis, more tests should be performed, both on the already tested wells (with different test parameters) and in other locations. The matter of selecting the most advantageous BHE design and construction in terms of test results has not been determined conclusively.
- The best effective thermal conductivity λ_{eff} result is observed for the BHE with a single U-pipe with gravel as the grout, for the classic method, and its value equals $2802 \text{ W}\cdot\text{K}^{-1}\cdot\text{m}^{-1}$. For the constant borehole resistivity method, the F1 exchanger (double U-pipe) has the best result ($2.724 \text{ W}\cdot\text{K}^{-1}\cdot\text{m}^{-1}$). However, according to the point-based method, the F2 exchanger (single U-pipe) turns out to be the best borehole heat exchanger. These values are considered to be very high, which suggests the potential for very efficient results of the heat pump operation for the given geological structure.
- The LG-4a borehole (BHE with a single U-pipe with gravel as the grout) has the best thermal resistance, at $0.045 \text{ K}\cdot\text{m}\cdot\text{W}^{-1}$ for the classic method. For the point-based and the constant borehole resistivity methods, the results indicate that the LG-3a borehole heat exchanger has the lowest thermal resistance.
- To compare the influence of the BHE construction on the thermal conductivity and resistance coefficient characteristics, one can use the Folsz boreholes, where one of the designs is a single U-tube and the other a double U-tube. In this case, it is clear that a single U-tube achieves better thermal resistance values, while a double U-tube achieves better conductivity. In industrial practice, a double U-tube is considered a better, albeit more expensive, design. However, many parameters can influence TRT results. One of the important factors for the borehole thermal resistance R_b is the sealing effectiveness (even and precise distribution of the grout). With a double U-tube, sealing/filling the borehole is more difficult than with a single U-tube.
- The new method for determining the characteristic coefficients from the thermal response test gives different results compared to the old (classic) method. The largest standard deviation for thermal conductivity can be observed in the LG-4a well, where it was as high as $0.397 \text{ W}\cdot\text{m}^{-1}\cdot\text{K}^{-1}$. The values of the remaining standard deviations are much lower, which may indicate a good relationship between thermal conductivity calculations for both methods. Thermal resistance is also characterized by small standard deviations. However, with the LG-4a well it can be seen that there may be significant differences in individual cases, most likely depending on the thermal response test duration.
- The constant thermal resistivity method provides outcomes that do not depend in any way on the test duration. Therefore, it can be theorized that it may be a more reliable and accurate method, yielding better borehole heat exchanger coefficients from the thermal response test (λ_{eff} and R_b). However, this is speculative and it must be supported by a greater number of measurements than currently are available to be conclusive. This is the subject of future work being carried out in borehole heat exchanger fields B and C of the AGH UST Geoenergetics Laboratory.
- Further research on the centric design of the BHE is merited. Theoretically, the centric design should be the most advantageous (the lowest R_b value), but simultaneously it is the most difficult to properly seal with filling material. Hence, practical problems may indicate that this type of design should not be used. It is, however, the most advantageous in terms of heat carrier hydraulics and must be used in deep BHEs.

The research has two key aspects. First, it compares various BHE constructions and identifies the best in terms of efficiency for the same geological conditions. Second, the quality of thermal response test results is checked. Both of these topics require further research using the methodology presented in the paper, and such research is being undertaken currently by the present authors.

Author Contributions: Conceptualization, A.S.-Ś., T.S. and P.L.; methodology, T.S. and M.A.R.; software, P.L.; validation, T.S. and P.L.; formal analysis, T.S. and P.L.; investigation, P.L.; resources, T.S. and P.L.; data curation, T.S. and A.S.-Ś.; writing—original draft preparation, T.S. and P.L.; writing—review and editing, M.A.R. and A.S.-Ś.; visualization, P.L.; supervision, T.S.; project administration, T.S.; funding acquisition, T.S. All authors have read and agreed to the published version of the manuscript.

Funding: This research received no external funding.

Institutional Review Board Statement: Not applicable.

Informed Consent Statement: Not applicable.

Data Availability Statement: Not applicable.

Acknowledgments: The research leading to these results has received funding from the Norway Grants 2014–2021 via the National Centre for Research and Development in Warsaw. The research project was also supported by the program “Excellence initiative—research university” for the AGH University of Science and Technology. Students from the Student Scientific Organization GEOWIERT participated in the research. They implemented the Rector’s grant obtained at AGH UST in the academic year 2020/2021.

Conflicts of Interest: The authors declare no conflict of interest.

Nomenclature

ΔT_i	Difference between feed temperature and return temperature for record i (K).
α	Ground thermal diffusivity ($\text{m}^2 \cdot \text{s}^{-1}$).
γ	Euler constant ($\gamma = 0.5772156$).
λ	Ground thermal conductivity ($\text{W} \cdot \text{m}^{-1} \cdot \text{K}^{-1}$).
λ_{cm}	Ground thermal conductivity (classic method) ($\text{W} \cdot \text{K}^{-1} \cdot \text{m}^{-1}$).
λ_{pm}	Ground thermal conductivity (point method) ($\text{W} \cdot \text{K}^{-1} \cdot \text{m}^{-1}$).
λ_{cbrm}	Ground thermal conductivity (constant borehole resistivity method) ($\text{W} \cdot \text{K}^{-1} \cdot \text{m}^{-1}$).
ρ	Density of rocks ($\text{kg} \cdot \text{m}^{-3}$).
ρ_i	Density of heat carrier for record i , which is dependent on temperature $\rho_i = f(T)$ ($\text{kg} \cdot \text{m}^{-3}$).
H	Borehole heat exchanger depth (m).
P	Thermal power (W).
P_{chi}	Temporary heating power for record i (W).
R_{b-cm}	Borehole thermal resistance (classic method) ($\text{K} \cdot \text{m} \cdot \text{W}^{-1}$).
R_{b-pm}	Borehole thermal resistance (point-based method) ($\text{K} \cdot \text{m} \cdot \text{W}^{-1}$).
R_{b-cbrm}	Borehole thermal resistance (constant borehole resistivity method) ($\text{K} \cdot \text{m} \cdot \text{W}^{-1}$).
T_0	Average natural temperature of geological profile of the borehole (K).
T_f	Feed temperature (K).
T_r	Return temperature (K).
$T(t_1)$	Average heat carrier temperature at time t_1 (K).
$T(t_2)$	Average heat carrier temperature at time t_2 (K).
T_z	Inlet temperature (at the inflow to the borehole heat exchanger) (K).
T_p	Return temperature (at the outflow of the borehole heat exchanger) (K).
$T_{sr(reg)}$	Temperature from the linear regression function ($T(t_1)$ or $T(t_2)$) (K).
\dot{V}, Q	Heat carrier flow rate ($\text{m}^3 \cdot \text{s}^{-1}$).
\dot{V}_i	Heat carrier flow rate for record i ($\text{m}^3 \cdot \text{s}^{-1}$).
c_i	Specific heat of heat carrier for record i , which is dependent on temperature $c_i = f(T)$ ($\text{J} \cdot \text{kg}^{-1} \cdot \text{K}^{-1}$).
c_v	Volumetric specific heat ($\text{J} \cdot \text{m}^{-3} \cdot \text{K}^{-1}$).
k	Coefficient of inclination of (straight) lines of trends, representing the function of the heat carrier temperature vs. the natural logarithm of time of TRT.
k_{cm}	Slope of regression line (classic method).
k_{pm}	Slope of regression line (point-based method).
k_{cbrm}	Slope of regression line (constant borehole resistivity method).
n	Number of records registered during the heating phase of the TRT.

q	Unit heat loss rate for borehole heat exchanger ($\text{W}\cdot\text{m}^{-1}$).
r	Radius (m).
r_b	Borehole radius (m).
u	Auxiliary variable.
t	Time (s).
t_1	Starting time (s).
t_2	Ending time (s).

References

1. Qian, X.; Yang, Y.; Lee, S.W. Design and Evaluation of the Lab-Scale Shell and Tube Heat Exchanger (STHE) for Poultry Litter to Energy Production. *Processes* **2020**, *8*, 500. [[CrossRef](#)]
2. Zhang, C.; Chen, P.; Liu, Y.; Sun, S.; Peng, D. An improved evaluation method for thermal performance of borehole heat exchanger. *Renew. Energy* **2015**, *77*, 142–151. [[CrossRef](#)]
3. Qian, X.; Lee, S.W.; Yang, Y. Heat Transfer Coefficient Estimation and Performance Evaluation of Shell and Tube Heat Exchanger Using Flue Gas. *Processes* **2021**, *9*, 939. [[CrossRef](#)]
4. Nordell, B. Borehole Heat Store Design Optimization. Ph.D. Thesis, Division of Water Resources Engineering, Luleå University of Technology, Luleå, Sweden, 1994.
5. Bujok, P.; Klempa, M.; Koziorek, J.; Rado, R.; Porzer, M. Evaluation of influence of climate conditions on rock mass energy balance in the research area of VSB—TU Ostrava. *AGH Drill. Oil Gas* **2012**, *29/1*, 97–107.
6. Koohi-Fayegh, S.; Rosen, M.A. Examination of thermal interaction of multiple vertical ground heat exchangers. *Appl. Energy* **2012**, *97*, 962–969. [[CrossRef](#)]
7. Schüppler, S.; Zorn, R.; Steger, H.; Blum, P. Uncertainty analysis of wireless temperature measurement (WTM) in borehole heat exchangers. *Geothermics* **2021**, *90*, 102019. [[CrossRef](#)]
8. Cassaso, A.; Sethi, R. Sensitivity analysis on the performance of a ground source heat pump equipped with a double U-pipe borehole heat exchanger. *Energy Procedia* **2014**, *59*, 301–308. [[CrossRef](#)]
9. Drysdale, R. Thermal Performance and Sustainability of Borehole Heat Exchangers within Building Clusters. Master's Thesis, The University of Western Ontario, London, ON, Canada, 2019.
10. Pollard, H.J.; Lee, F. Long term monitoring of borehole temperature profiles using a thermistor array in the Ball State University ground-source geothermal system. In Proceedings of the Conference 50th Annual GSA North-Central Section Meeting, Champaign, IL, USA, 18 April 2016.
11. Dijkshoorn, L.; Speer, S.; Pechnig, R. Measurements and Design Calculations for a Deep Coaxial Borehole Heat Exchanger in Aachen, Germany. *Int. J. Geophys.* **2013**, *2013*, 916541. [[CrossRef](#)]
12. Gehlin, S.; Andersson, O.; Bjelm, L.; Alm, P.G.; Rosberg, J.E. Country Update for Sweden. In Proceedings of the World Geothermal Congress 2015, Melbourne, Australia, 16–24 April 2015.
13. Hellstrom, G. *Ground Heat Storage Thermal Analyses of Duct Storage Systems Theory*; Dept. of Mathematical Physics, University of Lund: Lund, Sweden, 1991.
14. Eskilson, P. *Thermal Analysis of Heat Extraction Boreholes*; Dept. of Mathematical Physics, University of Lund: Lund, Sweden, 1987.
15. Rybach, L.; Eugster, W.J. Sustainability aspects of geothermal heat pump operation, with experience from Switzerland. *Geothermics* **2010**, *39*, 365–369. [[CrossRef](#)]
16. Rybach, L.; Hopkirk, R.J. *Experience with Borehole Heat Exchangers in Switzerland*; Institute of Geophysics ETH-Hoenggerberg: Zurich, Switzerland, 1994.
17. Weber, J.; Ganz, B.; Schellschmidt, R.; Sanner, B.; Schulz, R. Geothermal Energy Use in Germany. In Proceedings of the World Geothermal Congress 2015, Melbourne, Australia, 16–24 April 2015.
18. Schulte, D.O. Modeling insulated borehole heat exchangers. *Environ. Earth Sci.* **2016**, *75*, 910. [[CrossRef](#)]
19. Kurevija, T.; Macenić, M.; Sabolić, T.; Jovanović, D. Defining geoexchange extraction rates in the same geological environment for different borehole geometry settings—Pilot results from the happen—Horizon 2020 project. *Min.-Geol.-Pet. Eng. Bull.* **2021**, *36*, 99–113. [[CrossRef](#)]
20. Raymond, J.; Malo, M.; Tanguay, D.; Grasby, S.; Bakhteyar, F. Direct Utilization of Geothermal Energy from Coast to Coast: A Review of Current Applications and Research in Canada. In Proceedings of the World Geothermal Congress 2015, Melbourne, Australia, 16–24 April 2015.
21. Giordano, N. Efficiency evaluation of borehole heat exchangers in Nunavik, Québec, Canada. In Proceedings of the 25th International Congress of Refrigeration, Montréal, QC, Canada, 24–30 August 2019.
22. Boyd, T.L.; Sifford, A.; Lund, J.W. The United States of America Country Update 2015. In Proceedings of the World Geothermal Congress 2015, Melbourne, Australia, 16–24 April 2015; pp. 1–12.
23. Cortes, D.; Nasirian, A.; Dai, S. Smart Ground-Source Borehole Heat Exchanger Backfills: A Numerical Study: SEG-2018. In *Energy Geotechnics*; Ferrari, A., Laloui, L., Eds.; Springer Series in Geomechanics and Geoenvironment; Springer: Berlin/Heidelberg, Germany, 2019; pp. 27–34.

24. Sasada, M. Geothermal heat pumps in Japan. In *Proceedings of the Japan International Geothermal Symposium*; Geothermal Research Society of Japan: Tokyo, Japan, 2012; Available online: [http://www.geothermal-energy.org/pdf/IGAstandard/Japan/2012/p17-Masakatsu_Sasada\(Eng-Jpn\).pdf?](http://www.geothermal-energy.org/pdf/IGAstandard/Japan/2012/p17-Masakatsu_Sasada(Eng-Jpn).pdf?) (accessed on 27 June 2021).
25. Fang, L.; Diao, N.; Shao, Z.; Cui, P.; Zhu, K.; Fang, Z. Thermal analysis models of deep borehole heat exchangers. In *Proceedings of the IGSHA Research Track 2018*, Stockholm, Sweden, 18–20 September 2018; International Ground Source Heat Pump Association: Springfield, IL, USA, 2018.
26. Javadi, H.; Ajatrostaghi, S.; Rosen, M.A.; Pourfallah, M.A. Comprehensive Review of Backfill Materials and Their Effects on Ground Heat Exchanger Performance. *Sustainability* **2018**, *10*, 4486. [[CrossRef](#)]
27. Walch, A. Quantifying the technical geothermal potential from shallow borehole heat exchangers at regional scale. *Renew. Energy* **2020**, *165*, 369–380. [[CrossRef](#)]
28. Caulk, R.; Tomac, I. Reuse of Abandoned Oil and Gas Wells for Geothermal Energy Production. *Renew. Energy* **2017**, *112*, 388–397. [[CrossRef](#)]
29. Pan, S.; Kong, Y.; Chen, C.; Pang, Z.; Wang, J. Optimization of the utilization of deep borehole heat exchangers. *Geotherm. Energy* **2020**, *8*, 6. [[CrossRef](#)]
30. Sliwa, T.; Rosen, M.A. Natural and artificial methods for regeneration of heat resources for borehole heat exchangers to enhance the sustainability of underground thermal storages: A review. *Sustainability* **2015**, *7*, 13104–13125. [[CrossRef](#)]
31. Beier, R.A.; Acuña, J.; Mogensen, P.; Palm, B. Borehole resistance and vertical temperature profiles in coaxial borehole heat exchangers. *Appl. Energy* **2013**, *102*, 665–675. [[CrossRef](#)]
32. Zarrella, A.; De Carli, M. Heat transfer analysis of short helical borehole heat exchangers. *Appl. Energy* **2013**, *102*, 1477–1491. [[CrossRef](#)]
33. Zarrella, A.; Capozza, A.; De Carli, M. Analysis of short helical and double U-tube borehole heat exchangers: A simulation-based comparison. *Appl. Energy* **2013**, *112*, 358–370. [[CrossRef](#)]
34. Li, M.; Lai, A.C.K. Heat-source solutions to heat conduction in anisotropic media with application to pile and borehole ground heat exchangers. *Appl. Energy* **2012**, *96*, 451–458. [[CrossRef](#)]
35. Barbaresi Maioli, V.; Bovo, M.; Tinti, F.; Torreggiani, D.; Tassinari, P. Application of basket geothermal heat exchangers for sustainable greenhouse cultivation. *Renew. Sustain. Energy Rev.* **2020**, *129*, 109928. [[CrossRef](#)]
36. Sliwa, T.; Kucper, M. Accessing Earth’s heat using Geothermal Radial Drilling for borehole heat exchangers. *AGH Drill. Oil Gas* **2017**, *34*, 495–512. [[CrossRef](#)]
37. Mendrinós, D.; Katsantonis, S.; Karytsas, C. Pipe materials for borehole heat exchangers. In *Proceedings of the European Geothermal Congress 2016 (EGC2016)*, Strasbourg, France, 19–23 September 2016.
38. Sliwa, T.; Gawel, M. Ohorona atmosfernogo povitrâ zavdâki vikoristannâ vidnovlûvanih dzerel energii v sistemah opalennâ ta oholodzhennâ u gromads’kih ob’ektah u gmîni Palechnica. In *Improvement of Energy Management in Typical Public Buildings of the City and Oblast Ivano-Frankivsk*; Good Polish Practices of Utilizing Energy Saving in Infrastructural Facilities, Kraków–Zakopane, 9–12 September 2013; AGH University of Science and Technology: Kraków, Poland, 2013; pp. 1–11.
39. Gonet, A.; Sliwa, T.; Złotkowski, A.; Sapińska-Sliwa, A.; Macuda, J. The Analysis of Expansion Thermal Response Test (TRT) for Borehole Heat Exchangers (BHE). In *Proceedings of the Thirty-Seventh Workshop on Geothermal Reservoir Engineering*, Stanford, CA, USA, 30 January–1 February 2012; Stanford University: Stanford, CA, USA, 2012; p. 194.
40. Alberti, L.; Angelotti, A.; Antelmi, M.; La Licata, I. A Numerical Study on the Impact of Grouting Material on Borehole Heat Exchangers Performance in Aquifers. *Energies* **2017**, *10*, 703. [[CrossRef](#)]
41. Yoon, S.; Lee, S.R.; Xue, J.; Zosseder, K.; Go, G.H.; Park, H. Evaluation of the Thermal Efficiency and a Cost analysis of Different Types of Ground Heat Exchangers in Energy Piles. *Energy Convers. Manag.* **2015**, *105*, 393–402. [[CrossRef](#)]
42. Lund, J.W.; Toth, A.N. Direct Utilization of Geothermal Energy 2020 Worldwide Review. In *Proceedings of the World Geothermal Congress 2020*, Reykjavik, Iceland, 26 April–2 May 2020; International Geothermal Association: San Francisco, CA, USA, 2020.
43. Lund, J.W.; Gawell, K.; Boyd, T.L.; Jennejohn, D. The United States of America Country Update 2010. In *Proceedings of the World Geothermal Congress 2010*, Bali, Indonesia, 25–30 April 2010; pp. 1–18.
44. Lee, K.S. *Underground Thermal Energy Storage*; Springer Science & Business Media: Berlin/Heidelberg, Germany, 2012; p. 152.
45. Morita, K.; Bollmeier, S.W.; Mizogami, H. An experiment to prove the concept of the downhole coaxial heat exchanger (DCHE) in Hawaii. *Geotherm. Resour. Counc. Trans.* **1992**, *16*, 9–17.
46. Morita, K.; Matsubayashi, O.; Kusunoki, K. Down-hole coaxial heat exchanger using insulated inner pipe for maximum heat extraction. *Geotherm. Resour. Counc. Trans.* **1985**, *9*, 17–23.
47. Schneider, D.; Strothöffer, T.; Broßmann, E. Die 2800 m von Prenzlau oder die tiefste Erdwärmesonde der Welt. *Geotherm. Energ.* **1996**, *16*, 10–12.
48. Clauser, C. *Numerical Simulation of Reactive Flowing Hot Aquifers*; Springer: Berlin/Heidelberg, Germany, 2003.
49. Rybach, L.; Eugster, W. Reliable long term performance of BHE systems and market penetration—The Swiss success story. In *Proceedings of the 2nd Stockton International Geothermal Conference 1998*, Galloway, NJ, USA, 16–17 March 1998; pp. 41–57.
50. Rybach, L.; Hopkirk, R.J. Shallow and Deep Borehole Heat Exchangers—Achievements and Prospects. In *Proceedings of the World Geothermal Congress 1995*, Florence, Italy, 18–31 May 1995; pp. 2133–2138.
51. Kohl, T.; Salton, M.; Rybach, L. Data Analysis of the Deep Borehole Heat Exchanger Plant Weissbad (Switzerland). In *Proceedings of the World Geothermal Congress 2000*, Kyushu-Tohoku, Japan, 28 May–10 June 2000; pp. 3459–3464.

52. Kohl, T.; Brenni, R.; Eugster, W. System performance of a deep borehole heat exchanger. *Geothermics* **2002**, *31*, 687–708. [[CrossRef](#)]
53. Signorelli, S.; Andenmatten Bertoud, N.; Kohl, T.; Rybach, L. *Projekt Statistik Geothermische Nutzung der Schweiz für die Jahre 2002 und 2003*; Geowatt AG: Zürich, Switzerland, 2004.
54. Signorelli, S.; Wagner, R.; Kohl, T.; Rybach, L. *Statistik der Geothermischen Nutzung in der Schweiz, Überarbeitung der Geothermiestatistik von 1990 bis 2006*; Geowatt AG: Zürich, Switzerland, 2014.
55. Sliwa, T.; Kotyza, J. Selection of Optimal Construction of Borehole Heat Exchangers Based on Jachowka 2K Well to a Depth 2870 m. In *Methodology and Technology of Obtaining Usable Energy from a Single Geothermal Borehole*; Sokolowski, J., Ed.; Instytut Gospodarki Surowcami Mineralnymi i Energia PAN, Pracownia Geosynoptyki i Geotermii: Krakow, Poland, 2000; pp. 251–284. (In Polish)
56. Sokolowski, J.; Ludwikowski, B.; Pawlik, E. On the necessity to evaluate geothermal resources in counties lying within the small Poland and Silesia voivodeships. *Techn. Posz.* **1999**, *2*, 17–23. (In Polish)
57. Deng, J.; Wei, Q.; He, S.; Liang, M.; Zhang, H. What Is the Main Difference between Medium-Depth Geothermal Heat Pump Systems and Conventional Shallow-Depth Geothermal Heat Pump Systems? Field Tests and Comparative Study. *Appl. Sci.* **2019**, *9*, 5120. [[CrossRef](#)]
58. Sapińska-Sliwa, A.; Rosen, M.A.; Gonet, A.; Sliwa, T. Deep Borehole Heat Exchangers—A Conceptual and Comparative Review. *Int. J. Air-Cond. Refrig.* **2016**, *24*, 1630001. [[CrossRef](#)]
59. Gehlin, S. Thermal Response Test, Method Development and Evaluation. Ph.D. Thesis, Luleå University of Technology, Luleå, Sweden, 2002.
60. Gonet, A.; Sliwa, T.; Stryczek, S.; Sapińska-Sliwa, A.; Jaszczur, M.; Pająk, L.; Złotkowski, A. *Metodyka Identyfikacji Potencjału Ciepłego Górotworu wraz z Technologią Wykonywania i Eksploatacji Otworowych Wymienników Ciepła (Methodology for the Identification of Potential Heat of the Rock Mass along with Technology Implementation and Operation of the Borehole Heat Exchangers)*; Wydawnictwa AGH: Kraków, Poland, 2011. (In Polish)
61. Sliwa, T. *Badania Podziemnego Magazynowania Ciepła za Pomocą Kolektorów Słonecznych i Wymienników Otworowych Ciepła (Research on Underground Thermal Energy Storage by Use Solar Collectors and Borehole Heat Exchangers)*; Wydawnictwa AGH: Kraków, Poland, 2012.
62. Czekalski, D.; Obstawski, P. Procedura testowania pionowego wymiennika gruntowego w warunkach eksploatacyjnych. *Cieplownictwo Ogrzew. Went.* **2006**, *37/4*, 18–21. (In Polish)
63. Gonet, A.; Sliwa, T. Thermal response test on example of borehole heat exchangers in Ecological Park of Education and Amusement “OSSA”. In *Proceedings of the XIV International Scientific-Technical Conference “New Knowledge in the Area of Drilling, Production, Transport and Storage Hydrocarbons”*; Technická Univerzita Kosice: Kosice, Slovakia, 2008; pp. 42–47.
64. Sapińska-Sliwa, A.; Sliwa, T.; Twardowski, K.; Szymiski, K.; Gonet, A.; Żuk, P. Method of Averaging the Effective Thermal Conductivity Based on Thermal Response Tests of Borehole Heat Exchangers. *Energies* **2020**, *13*, 3737. [[CrossRef](#)]
65. Luo, J.; Tuo, J.; Huang, H.; Zhu, Y.Q.; Jiao, Y.Y.; Xiang, W.; Rohn, J. Influence of groundwater levels on effective thermal conductivity of the ground and heat transfer rate of borehole heat exchangers. *Appl. Therm. Eng.* **2018**, *128*, 508–516. [[CrossRef](#)]
66. Zhang, C.; Xu, H.; Fan, J.; Sun, P.; Sun, S.; Kong, X. The coupled two-step parameter estimation procedure for borehole thermal resistance in thermal response test. *Renew. Energy* **2020**, *154*, 672–683. [[CrossRef](#)]
67. Rybach, L. *Shallow Systems*; Geowatt AG: Zurich, Switzerland, 2012.
68. Spitler, J.; Gehlin, S. Thermal response testing for ground source heat pump systems—An historical review. *Renew. Sustain. Energy Rev.* **2015**, *50*, 1125–1137. [[CrossRef](#)]
69. Badenes, B.; Mateo Pla, M.Á.; Lemus-Zúñiga, L.G.; Sáiz Mauleón, B.; Urchueguía, J.F. On the Influence of Operational and Control Parameters in Thermal Response Testing of Borehole Heat Exchangers. *Energies* **2017**, *10*, 1328. [[CrossRef](#)]
70. Perina, T. Derivation of the Theis (1935) Equation by Substitution. *Ground Water* **2010**, *48*, 6–7. [[CrossRef](#)]
71. Sliwa, T.; Sojczyńska, A.; Rosen, M.A.; Kowalski, T. Evaluation of temperature profiling quality in determining energy efficiencies of borehole heat exchangers. *Geothermics* **2019**, *78*, 129–137. [[CrossRef](#)]
72. Sapińska-Sliwa, A.; Rosen, M.A.; Gonet, A.; Kowalczyk, J.; Sliwa, T. A New Method Based on Thermal Response Tests for Determining Effective Thermal Conductivity and Borehole Resistivity for Borehole Heat Exchangers. *Energies* **2019**, *12*, 1072. [[CrossRef](#)]
73. Pawlikowski, B. *Dokumentacja Geologiczna Wierceń dla Przyszłej Instalacji Otworowych Wymienników ciepła w Celach Naukowo-Badawczych*; AGH: Kraków, Poland, 2008. (In Polish)
74. Sliwa, T.; Sapińska-Sliwa, A.; Knez, D.; Bieda, A.; Kowalski, T.; Złotkowski, A. *Borehole Heat Exchangers: Production and Storage of Heat in the Rock Mass*; Laboratory of Geoenergetics book series; Drilling, Oil and Gas Foundation: Kraków, Poland, 2016; Volume 2, p. 175.
75. Sliwa, T.; Gonet, A. Otworowe wymienniki ciepła jako źródło ciepła lub chłodu na przykładzie Laboratorium Geoenergetyki WVNIG AGH (Borehole heat exchangers as heat or cool source on the basis of Laboratory of Geoenergetics of Drilling, Oil and Gas Faculty in AGH University of Science and Technology). *Wiert. Naft. Gaz* **2011**, *28*, 419–430. (In Polish)
76. Sanner, B.; Hellström, G.; Spitler, J.; Gehlin, S. Thermal Response Test—Current Status and World-Wide Application. In *Proceedings of the World Geothermal Congress 2005*, Antalya, Turkey, 24–29 April 2005.
77. Lamarche, L.; Raymond, J.; Pambou, C.H. Evaluation of the Internal and Borehole Resistances during Thermal Response Tests and Impact on Ground Heat Exchanger Design. *Energies* **2018**, *11*, 38. [[CrossRef](#)]

78. Sapińska-Śliwa, A. *Efektywność Pozyskiwania Ciepła z Górotworu w Aspekcie Sposobu Udostępniania Otworami Wiertniczymi (Effectiveness of Heat Recovery from Rock Mass in the Context of the Production Method by Means of Boreholes)*; Rozprawy Monografie Number 364; Wydawnictwa AGH: Kraków, Poland, 2019; p. 319. (In Polish)
79. Grygieńcza, A. *Analiza Metod Oceny Mocy Grzewczej Otworowych Wymienników Ciepła (Analysis of Estimation Methods of Borehole Heat Exchangers Power Rating)*. Master's Thesis, AGH University of Science and Technology, Drilling, Oil and Gas Faculty, Krakow, Poland, 2009. (In Polish).